

# **Feasibility of Using Wavewatch III for Days-Ahead Output Forecasting for Grid Connected Wave Energy Projects in Washington and Oregon**

*Stage Gate #2 Final report*

**EPRI-WP-012**

---



# **Feasibility of Using Wavewatch III for Days-Ahead Output Forecasting for Grid Connected Wave Energy Projects in Washington and Oregon**

*Stage Gate #2 Final report*

**EPRI-WP-012**

February 29, 2008

EPRI Project Manager

Roger Bedard

## **DISCLAIMER OF WARRANTIES AND LIMITATION OF LIABILITIES**

THIS DOCUMENT WAS PREPARED BY THE ORGANIZATION(S) NAMED BELOW AS AN ACCOUNT OF WORK SPONSORED OR COSPONSORED BY THE ELECTRIC POWER RESEARCH INSTITUTE, INC. (EPRI). NEITHER EPRI, ANY MEMBER OF EPRI, ANY COSPONSOR, THE ORGANIZATION(S) BELOW, NOR ANY PERSON ACTING ON BEHALF OF ANY OF THEM:

(A) MAKES ANY WARRANTY OR REPRESENTATION WHATSOEVER, EXPRESS OR IMPLIED, (I) WITH RESPECT TO THE USE OF ANY INFORMATION, APPARATUS, METHOD, PROCESS, OR SIMILAR ITEM DISCLOSED IN THIS DOCUMENT, INCLUDING MERCHANTABILITY AND FITNESS FOR A PARTICULAR PURPOSE, OR (II) THAT SUCH USE DOES NOT INFRINGE ON OR INTERFERE WITH PRIVATELY OWNED RIGHTS, INCLUDING ANY PARTY'S INTELLECTUAL PROPERTY, OR (III) THAT THIS DOCUMENT IS SUITABLE TO ANY PARTICULAR USER'S CIRCUMSTANCE; OR

(B) ASSUMES RESPONSIBILITY FOR ANY DAMAGES OR OTHER LIABILITY WHATSOEVER (INCLUDING ANY CONSEQUENTIAL DAMAGES, EVEN IF EPRI OR ANY EPRI REPRESENTATIVE HAS BEEN ADVISED OF THE POSSIBILITY OF SUCH DAMAGES) RESULTING FROM YOUR SELECTION OR USE OF THIS DOCUMENT OR ANY INFORMATION, APPARATUS, METHOD, PROCESS, OR SIMILAR ITEM DISCLOSED IN THIS DOCUMENT.

ORGANIZATION(S) THAT PREPARED THIS DOCUMENT

**Virginia Polytechnical Institute and State University— Advanced Research Institute**

## **NOTE**

Electric Power Research Institute, EPRI, and TOGETHER...SHAPING THE FUTURE OF ELECTRICITY are registered service marks of the Electric Power Research Institute, Inc.

Copyright © 2007 Electric Power Research Institute, Inc. All rights reserved.

# CITATIONS

This document was prepared by

Virginia Tech Advanced Research Institute  
4300 Wilson Blvd., Suite 750  
Arlington, VA 22203

Principal Investigator  
George Hagerman

This publication is a corporate document that should be cited in the literature in the following manner:

*Title of Document: Subtitle.* EPRI, Palo Alto, CA <Year.> <Product ID Number>.



# ABSTRACT

The overall goal of this feasibility study was to evaluate ocean wave energy predictability time frames and associated accuracies and to define the requirements for an operational wave energy forecasting workstation that will enhance the assimilation of wave energy into the utility grid, increasing its market value to the Federal Columbia River Power and Transmission System.

In order to achieve those goals, this study has the following specific objectives:

- (1) Evaluated the forecast skill of NOAA's operational WAVEWATCH III model in comparison with buoy-measured wave data in deep water off Washington and Oregon
- (2) Identified and evaluated appropriate measurement-to-measurement correlations that can be used to extend the "reach" of WAVEWATCH to potential wave power plant locations that do not coincide with operational WAVEWATCH III output locations
- (3) Determined the potential benefit to this model of incorporating retrospective ("looking back at the data") algorithms into a "self-training" neural network engine to evolve and improve its wave forecasting skill, and
- (4) Defined what must be done to program such a neural network engine and integrate it with the WAVEWATCH III model and incorporate the combined system into a real-time, operational forecasting workstation.





## **ACKNOWLEDGEMENTS**

EPRI would like to acknowledge the sponsorship of Bonneville Power Administration and the cofunding contributions of SAIC Maritime Technologies and Virginia Polytechnical Institute and State University.

The project technical work was performed by SAIC Maritime Technologies and the Virginia Tech Advanced Research Institute



# CONTENTS

|  |            |
|--|------------|
| <b>1 INTRODUCTION .....</b>  | <b>1-1</b> |
| 1.1. Required Forecast Accuracy.....   | 1-2        |
| 1.2. Required Forecast Time Horizons .....   | 1-4        |
| 1.3. Report Organization .....   | 1-5        |
| <b>2 DATA SOURCES .....</b>  | <b>2-1</b> |
| 2.1. WaveWatch III Forecast Wave Data .....  | 2-1        |
| 2.2. NDBC Measured Wave Data .....   | 2-3        |
| 2.3. CDIP Measured Wave Data .....   | 2-4        |
| <b>3 METHODOLOGY .....</b>   | <b>3-1</b> |
| 3.1. Evaluation of WaveWatch III Forecast Skill .....                              | 3-1        |
| 3.2. Correlation of Offshore and Coastal Wave Measurements.....                    | 3-3        |
| 3.3. Influence of Sea vs. Swell Dominance on Measurement Correlations .....        | 3-6        |
| <b>4 RESULTS .....</b>   | <b>4-1</b> |
| 4.1. Evaluation of WaveWatch III Forecast Skill .....                              | 4-1        |
| 4.2. Correlation of Offshore and Coastal wave Measurements .....                   | 4-10       |
| 4.3. Influence of Sea vs Swell Dominance on Coastal Measurement Correlations ..... | 4-11       |
| <b>5 CONCLUSIONS .....</b>   | <b>5-1</b> |
| <b>6 RECOMMENDATIONS FOR FUTURE WORK.....</b>                                      | <b>6-1</b> |
| <b>7 REFERENCES .....</b>  | <b>7-1</b> |
| <b>A PRIMER ON WAVE ENERGY VARIABILITY.....</b>                                    | <b>A-1</b> |
| <b>B SPECTRAL ANALYSIS AND SEA STATE PARAMETER ESTIMATION.....</b>                 | <b>B-1</b> |
| <b>C COMPLETE RESULTS FOR FORECAST AND MEASUREMENT CORRELATIONS.....</b>           | <b>C-1</b> |



# 1

## INTRODUCTION

The overall goal of this feasibility study is to evaluate ocean wave energy predictability time frames and associated accuracies and to define the requirements for an operational wave energy forecasting workstation that will enhance the assimilation of wave energy into the utility grid, increasing its market value to the Federal Columbia River Power and Transmission System.

Rather than develop any sort of new wave forecast tool “from scratch,” EPRI chose to evaluate an existing wave prediction model, namely WAVEWATCH III, which is routinely used by the National Oceanic and Atmospheric Administration (NOAA) for marine weather forecasting and the U.S. Navy for fleet operations planning.

This study has the following specific objectives:

- (1) Evaluate the forecast skill of NOAA’s operational WAVEWATCH III model in comparison with buoy-measured wave data in deep water off Washington and Oregon
- (2) Identify and evaluate appropriate measurement-to-measurement correlations that can be used to extend the “reach” of WAVEWATCH to potential wave power plant locations that do not coincide with operational WAVEWATCH III output locations
- (3) Determine the potential benefit to this model of incorporating retrospective (“looking back at the data”) algorithms into a “self-training” neural network engine to evolve and improve its wave forecasting skill, and
- (4) Define what must be done to program such a neural network engine and integrate it with the WAVEWATCH III model and incorporate the combined system into a real-time, operational forecasting workstation.

In order to justify moving beyond this feasibility study, through Stage Gate #2, into a second phase project, we must answer the following questions:

- (A) Is the accuracy of existing, operational WAVEWATCH III forecasts sufficiently good that any further development of a forecasting workstation for wave energy utility integration purposes should be based on this NOAA operational product?
- (B) Is the correlation between locations where operational WAVEWATCH III forecasts are routinely available and the coastal locations where wave power plants would be sited and such forecasts and neural net technology may be used to extend the “reach” of WAVEWATCH forecasts into such locations?

In order to answer these questions, a forecast accuracy target must be established to define “sufficiently good.” That is the subject of Section 1.1, below, which first provides background information on the integration of intermittent renewable energy supply sources into utility grid

operation, and then proposes a forecast accuracy metric consistent with our present accuracy in specifying wave power plant output as a function of wave height and period parameters.

Also relevant is the time horizon for which “sufficiently good” forecasts are required. As explained in Section 1.2, having accurate forecasts out to 48 hours ahead would enable reliable scheduling of utility grid resources for balancing supply and demand, as well as establishing market confidence in generation schedules that would be furnished by wave energy project developers in day-ahead and two-day-ahead markets.

## **1.1. Required Forecast Accuracy**

The intermittent nature of wave power creates opportunities and challenges in grid integration and management of system reliability. As has been demonstrated with wind power, developing accurate forecasts can reduce operational grid integration issues. It also can lessen the need for other mitigating measures and their associated costs. As such, wave forecasting is expected to be an important tool for managing the variable nature of wave power and will be required to reliably increase wave energy penetration at some future time when a large amount of wave generation capacity may be connected to the Bonneville Power Administration’s grid.

It is envisioned that all wave power plants will forecast their output for the next day or two as well as one to three hours before the start of their contracted delivery hour, with specific times dictated by future operational policies and energy market conditions prevailing when wave power development has reached an aggregate installed capacity of several hundred to a few thousand megawatts, which is likely not to occur for at least a decade (however, it is likely that initial waves power plants to be installed over the next few years in Oregon and Washington will have a requirement to do wave forecasting).

The system controller will then incorporate both short-term (3 hours or less) and long-term (one or more days) forecasts into the operational plan to maintain supply and demand balance in the system control area while accommodating the expected output from wave power plants. Thus, accurate forecasts will improve the efficiency of planning and procuring regulating reserves and load/supply following services, as described below.

Regulating reserves are fast-responding resources that are used in real time to help maintain supply demand balance, typically within a 20-minute timeframe. Experience with wind power indicates that over timeframes less than 20 minutes, variability of net demand (considering variability of both load and wind together) increases only marginally with increasing wind penetration, suggesting that it can be reasonably managed with existing or relatively small increases in regulating reserves (Reference 1).

Due to the much greater inertia of water relative to air, wave conditions change more slowly than wind conditions. Therefore, it is expected that regulating reserves procured to address short-term load variability will be adequate to mitigate the effects of short-term wave variability over time scales of several tens of minutes.

The bigger reliability risk associated with large-scale wave power development is wave ramping that persists from tens of minutes to tens of hours, particularly when waves ramp in the opposite direction of system load; in other words, when waves pick up as electric power demand goes down, or vice versa. Load/supply following services are similar to regulating reserves, except that they are used to respond to changes in wind ramping that lasts hours to days.

Procurement of load/supply following services would be based on wave forecasts and associated wave forecasting accuracy standards, as likely would be applied to wave power interconnection agreements. Use or dispatch of load/supply following services would depend on which resources (additional supply, load-shedding services, or inter-control area dynamic exchange) would best meet technical operating or reliability requirements in the most cost-effective manner within established energy market rules.

At this very early stage of wave power development in the Pacific Northwest (and elsewhere), no standards have been established for wave forecasting accuracy. There thus exists no established metric against which to judge the accuracy of WAVEWATCH III operational forecasts for the planning and procurement of load/supply following services.

For purposes of this study, EPRI suggests that to be considered useful for utility grid integration of wave power, a wave forecasting tool should be at least as accurate as the wave energy project developers' ability to accurately specify the electrical output of a wave energy device as a function of wave height and period parameters. This requires a brief explanation of how this is done, which is given below.

Unlike wind turbine power curves, which specify wind turbine output power as a function of only one variable (wind speed), wave energy device power is a function of two sea state variables: a wave height parameter and a wave period parameter, and so the power curve is often referred to as a "power matrix." An example of such a power matrix is given in Table 1.1 for the Pelamis wave energy device.

Based on emerging wave energy device performance characterization protocols in Europe (References 3 and 4), such characterizations should use sea state bins with a wave height increment of 0.5 m and a period increment of 0.5 or 1.0 second. This suggests that as long as a wave forecast error is within  $\pm 0.25$  m for significant wave height and  $\pm 0.25$  sec for energy period, the degree of device output uncertainty associated with the forecast error is within the same degree of device output uncertainty as would exist with a perfect forecast.

Note in Table 1.1 that device power output changes much more dramatically between wave height bins than between wave period bins. Although this example power matrix is for the Pelamis wave energy device, the same trend holds true for other wave energy devices, due to the fact that the incident wave power per unit width of any device is proportional to the product of wave height squared and wave period. Therefore, sensitivity to wave height is much greater. For this reason, Reference 4 adopts a broader definition of the wave period bin increment (1.0 second) than Reference 3 (0.5 second). Therefore, EPRI suggests that a wave period forecast error of  $\pm 1.0$  seconds represents an appropriate accuracy goal for this feasibility study.

**Table 1-1****Wave power matrix for the 750 kW Pelamis prototype unit**

Wave power matrix for the 750 kW Pelamis prototype unit as tested at the European Marine Energy Centre in 2003 and installed off the coast of Portugal in the summer of 2007. Note that “power period” is the same as energy period, and this is the preferred sea state period characterization in emerging wave energy ocean test protocols.

|   | Power period ( $T_{pow}$ , s) |      |      |      |      |      |      |      |      |      |      |      |      |      |      |      |      |
|---|-------------------------------|------|------|------|------|------|------|------|------|------|------|------|------|------|------|------|------|
|   | 5.0                           | 5.5  | 6.0  | 6.5  | 7.0  | 7.5  | 8.0  | 8.5  | 9.0  | 9.5  | 10.0 | 10.5 | 11.0 | 11.5 | 12.0 | 12.5 | 13.0 |
| Significant wave height ( $H_{s,1g}$ , m) | 0.5                           | idle | idle | idle | idle | idle | idle | idle | idle | idle | idle | idle | idle | idle | idle | idle | idle |
|   | 1.0                           | idle | 22   | 29   | 34   | 37   | 38   | 37   | 35   | 32   | 29   | 26   | 23   | 21   | idle | idle | idle |
|   | 1.5                           | 32   | 50   | 65   | 76   | 83   | 86   | 83   | 78   | 72   | 65   | 59   | 53   | 47   | 42   | 37   | 33   |
|   | 2.0                           | 57   | 88   | 115  | 136  | 148  | 153  | 152  | 147  | 138  | 127  | 116  | 104  | 93   | 83   | 74   | 66   |
|   | 2.5                           | 89   | 138  | 180  | 212  | 231  | 238  | 230  | 216  | 199  | 181  | 163  | 146  | 130  | 116  | 103  | 92   |
|   | 3.0                           | 129  | 198  | 260  | 305  | 332  | 340  | 332  | 315  | 292  | 266  | 240  | 219  | 210  | 188  | 167  | 149  |
|   | 3.5                           | -    | 270  | 354  | 415  | 438  | 440  | 424  | 404  | 377  | 362  | 326  | 292  | 260  | 230  | 215  | 202  |
|   | 4.0                           | -    | -    | 462  | 502  | 540  | 546  | 530  | 499  | 475  | 429  | 384  | 366  | 339  | 301  | 267  | 237  |
|   | 4.5                           | -    | -    | 544  | 635  | 642  | 648  | 628  | 590  | 562  | 528  | 473  | 432  | 382  | 356  | 338  | 300  |
|   | 5.0                           | -    | -    | -    | 739  | 726  | 731  | 707  | 687  | 670  | 607  | 557  | 521  | 472  | 417  | 369  | 348  |
|   | 5.5                           | -    | -    | -    | 750  | 750  | 750  | 750  | 750  | 737  | 667  | 658  | 586  | 530  | 496  | 446  | 395  |
|   | 6.0                           | -    | -    | -    | -    | 750  | 750  | 750  | 750  | 750  | 750  | 711  | 633  | 619  | 558  | 512  | 470  |
|   | 6.5                           | -    | -    | -    | -    | 750  | 750  | 750  | 750  | 750  | 750  | 750  | 743  | 658  | 621  | 579  | 512  |
|   | 7.0                           | -    | -    | -    | -    | -    | 750  | 750  | 750  | 750  | 750  | 750  | 750  | 750  | 676  | 613  | 584  |
|   | 7.5                           | -    | -    | -    | -    | -    | -    | 750  | 750  | 750  | 750  | 750  | 750  | 750  | 750  | 686  | 622  |
|   | 8.0                           | -    | -    | -    | -    | -    | -    | -    | 750  | 750  | 750  | 750  | 750  | 750  | 750  | 750  | 690  |

Note that in future, more detailed forecasting studies, it might be appropriate to have a more stringent accuracy standard over regions of the power matrix where device performance is most sensitive to sea state changes, and less stringent accuracy standards where device performance changes only gradually with sea state changes. In the above Pelamis matrix, for example, a high forecast accuracy for significant wave heights of 1.0 m or less would make little difference, since the device is either idling or generating only 5% of its rated output under such conditions throughout the entire period range.

## 1.2. Required Forecast Time Horizons

As described above, wave energy forecasts would be used to optimize operational management of the utility grid, informing operator decisions about economic dispatch, unit commitment, hydro storage planning, and power exchanges with neighboring systems. The required forecast time horizon depends on the size of the system and the type of conventional units. For large interconnected systems with “slow” units (e.g. steam turbines), this is typically 48 to 72 hours (Reference 2).



Wave energy projects will be expected to meet their contracted generation schedules, while deviations from such schedules will incur financial penalties. Accurate wave forecasting would minimize the risk of such penalties. The time horizons of interest will be defined by prevailing market rules, but usually lie within 48 hours ahead (Reference 2).

Although not directly relevant to grid integration, it should be mentioned here that accurate wave forecasts for longer time horizons (i.e. 3 to 7 days ahead) will be useful for scheduling project installation activities, as well as offshore service visits for inspection, maintenance, and repairs. While climatology would be used for long-term planning of such activities months in advance, the day-to-day mobilization of equipment and personnel will require accurate forecasts up to a week in advance. This also is true for scheduling responses to any forced outage situations that will require previously unscheduled access offshore.

With potential uses for installation and maintenance in mind, this study evaluated forecast time horizons out to one week ahead. For utility grid integration purposes, however, the accuracy requirement of  $\pm 0.5$  m in significant wave height and  $\pm 1$  second in dominant wave period will be most useful if met out to a time horizon of 48 hours ahead.

### **1.3. Report Organization**

In Section 2 of this report we describe our data sources, and in Section 3, we summarize our analysis methodology. Section 4 presents our results, and Section 5 presents our conclusions. Section 6 makes recommendations for future work, and Section 7 provides a list of references.



# 2

## DATA SOURCES

The forecast data source for this project is an operational forecasting model developed by the National Environmental Prediction Centers (NECP) of the National Oceanic and Atmospheric Administration (NOAA), known as WAVEWATCH III. Routinely used for NOAA's marine weather forecasts, WAVEWATCH III has been adopted by the Fleet Numerical Oceanographic Center at Monterey to support U.S. Navy operations around the world, and is also used in hindcast mode by the U.S. Army Corps of Engineers for the design of coastal engineering projects such as piers and breakwaters. Section 2.1 describes the operational forecast products supplied by this model and used in our study.

The measured data sources for this project are moored-buoy stations maintained by the National Data Buoy Center (NDBC), and the Coastal Data Information Program (CDIP) operated by Scripps Institute of Oceanography. Although our original proposal included a northern wave measurement station (46206) operated by the Canadian Meteorological and Environmental Data Service, we were not able to download measured wave spectra for this station. Sections 2.1 and 2.2 describe the NDBC and CDIP measured wave data products used in our study.

### 2.1. WaveWatch III Forecast Wave Data

WAVEWATCH III is a third-generation wave forecast model derived from WAVEWATCH I, as developed at Delft University of Technology in the Netherlands, and WAVEWATCH II, as developed at NASA's Goddard Space Flight Center. WAVEWATCH III differs from its two predecessors in many important points, including governing equations, model structure, numerical computational methods and parameterization of wave physics.

Global ocean wave forecasts are produced at the NCEP by using WAVEWATCH III to generate directional wave spectra in 24 directions and 25 frequencies. Each directional spectrum consists of the sea surface variance density over 24 directions beginning at 90 degrees to the east, with a sector resolution of 15 degrees. The 25 frequency bins used by the model are given in Table 2-1. Model documentation and testing, as well as the availability of operational forecast products, are described at <http://polar.ncep.noaa.gov/waves/>.

Wave spectral data are computed on a 1.25 by 1.00 degree longitude/latitude grid for ocean points between latitude 78.0 degrees North to 78.0 degrees South. Wind fields are the only driving force used in the model and are constructed from spectral coefficients of the lowest sigma-layer winds from the NCEP analysis and forecasts of the Global Forecasting System (GFS) with no interpolation to the model grid required.

The winds are adjusted to a height of 10 m by using a logarithmic atmospheric boundary layer profile corrected for stability based on air- sea temperature differences. GFS wind fields are used

to produce wave forecasts at 3-hour intervals out to 180 hours ahead of the forecast issue date and time. WAVEWATCH III forecasts are issued four times daily at 0000, 0600, 1200 and 1800 Greenwich Mean Time (GMT).

**Table 2-1.**  
**WAVEWATCH spectral frequency bins and corresponding bandwidths.**

| Frequency Bin Number | Center Frequency (Hz) | Frequency Bandwidth (Hz) | Center Period (s) |
|----------------------|-----------------------|--------------------------|-------------------|
| 1                    | .0418                 | .00399                   | 23.94             |
| 2                    | .0459                 | .00439                   | 21.76             |
| 3                    | .0505                 | .00482                   | 19.79             |
| 4                    | .0556                 | .00531                   | 17.99             |
| 5                    | .0612                 | .00584                   | 16.35             |
| 6                    | .0673                 | .00642                   | 14.87             |
| 7                    | .0740                 | .00706                   | 13.51             |
| 8                    | .0814                 | .00777                   | 12.29             |
| 9                    | .0895                 | .00855                   | 11.17             |
| 10                   | .0985                 | .00940                   | 10.15             |
| 11                   | .1083                 | .01034                   | 9.23              |
| 12                   | .1192                 | .01138                   | 8.39              |
| 13                   | .1311                 | .01251                   | 7.63              |
| 14                   | .1442                 | .01376                   | 6.93              |
| 15                   | .1586                 | .01514                   | 6.30              |
| 16                   | .1745                 | .01666                   | 5.73              |
| 17                   | .1919                 | .01832                   | 5.21              |
| 18                   | .2111                 | .02015                   | 4.74              |
| 19                   | .2322                 | .02217                   | 4.31              |
| 20                   | .2555                 | .02438                   | 3.91              |
| 21                   | .2810                 | .02682                   | 3.56              |
| 22                   | .3091                 | .02951                   | 3.24              |
| 23                   | .3400                 | .03246                   | 2.94              |
| 24                   | .3740                 | .03570                   | 2.67              |
| 25                   | .4114                 | .03927                   | 2.43              |

The global-scale WAVEWATCH III model only provides the general wave pattern over the deep ocean. To predict wave conditions over the continental shelf and near land boundaries, a regional model having higher resolution grid is required.

Consequently, NOAA has developed a series of higher-resolution regional models, including the Eastern North Pacific (ENP) regional wave model used in our study. The global model described above provides the boundary conditions to the ENP model, whose domain extends from 170.25°W to 76.75°W and from 4.75°N to 62.25°N with a grid resolution of 0.25° by 0.25° in latitude and longitude. The ENP model has been operational since September 2001.

The following wind and wave parameters are available in gridded binary (GRIB) format for every point in the high-resolution ENP regional domain: significant wave height, peak wave period and direction, wind sea peak period and direction, wind speed and direction, and u- and v-wind components at an elevation of 10 m above sea level.

Directional wave spectra are operationally available only at certain data buoy stations. Five such WAVEWATCH output locations were used in this study, as described in Section 3.1.

## **2.2. NDBC Measured Wave Data**

The National Data Buoy Center (NDBC) deploys and maintains a variety of moored buoy platforms, including 3-m, 10-m, and 12-m diameter discus hulls, and 6-m long boat-shaped (NOMAD) hulls in coastal and offshore waters in longitudes ranging from the western Atlantic Ocean to the Pacific Ocean around Hawaii, and in latitudes ranging from the Bering Sea to the South Pacific. On an hourly basis, NDBC's moored buoys measure and transmit barometric pressure; the direction, average speed, and gust speed of local winds; air and sea temperatures; and wave energy spectra from which sea state parameters are calculated, including significant wave height, peak or dominant wave period, and average wave period.

Wave measurements are derived from accelerometers on board the buoys, which measure the heave acceleration or the vertical displacement of the buoy hull during the data acquisition time, which is either 20 or 40 minutes for buoys off the Pacific Northwest. A Fast Fourier Transform is applied to the accelerometer time series data by the processor on board the buoy to transform the data from the temporal domain into the frequency domain. Response amplitude operator processing is then performed on the transformed data to account for both hull and electronic noise and derive the non-directional wave spectrum.

NDBC wave measurement accuracy is reported at [www.ndbc.noaa.gov/rsa.shtml](http://www.ndbc.noaa.gov/rsa.shtml), which indicates that significant wave height is measured to within +/- 0.2 m, and dominant wave period is measured to within +/- 1 sec. Significant wave heights of less than 0.25 m are reported with zero height and period. Frequency resolution on wave measurement systems can vary from 0.005 Hz at low frequencies to 0.02 Hz at high frequencies. Note that in the analyses conducted for this report, our estimates of measured significant wave height, dominant wave period, and wave energy period were derived directly from the measured wave spectra. NDBC does not indicate the accuracy of its spectral measurements. Reference 5 reports that in 1,369 hourly wave records collected by Buoy 44 014 during August and September 1993, approximately 60% of the records had an upper bound rms error of less than 30% of the rms energy of the spectrum.

### **2.3. CDIP Measured Wave Data**

The Coastal Data Information Program (CDIP) is operated by the Ocean Engineering Research Group at Scripps Institution of Oceanography. The CDIP network has deployed and maintained wave gauging stations at well over 100 locations, mostly along the U.S. Pacific coast. CDIP wave buoy measurements are also derived from accelerometers inside the buoys. Unlike NDBC's buoys which serve as platforms for a variety of meteorological and oceanographic measurements, CDIP buoys are largely designed solely for wave measurements. Reference 6 reports the comparison of directional wave measurements among a CDIP Waverider buoy (manufactured by Datawell), a nearby NDBC 3-meter discus buoy, and an array of fixed wave gauges on the "Harvest" production platform off Point Conception, indicating similar performance for non-directional sea state parameters such as significant wave height and dominant wave period.

For further explanation of non-directional and directional wave spectra, and definition of sea state parameters such as significant wave height and peak wave period, see Appendix A.

# 3

## METHODOLOGY

Three major analyses were conducted for this study. The first analysis, described in Section 3.1, was to evaluate WAVEWATCH III forecast skill by comparing forecast and measured sea state parameters at different forecast time horizons. The second analysis, described in Section 3.2, was to characterize the correlation of measured sea state parameters between offshore and coastal data buoy stations, since it is such correlations that must be used to “extend the reach” of WAVEWATCH III to locations where its spectral forecast products are not available. The third analysis, described in Section 3.3, was to examine selected high-energy wave events to see how these correlations differ between events dominated by local wind seas and events dominated by swell from offshore storms.

### 3.1. Evaluation of WaveWatch III Forecast Skill

For this analysis, we used forecast and measured wave data for three near-shore NDBC stations that had good measured data recovery: 46029 (~70%), 46050 (100%), and 46022 (100%). To discover if there were significant differences in forecast skill between far offshore stations and the near-shore stations, we added two more NDBC stations to our study, both located hundreds of nautical miles offshore, in water depths of thousands of meters: 46005 and 46002. Both of these far offshore stations have 100% measured data availability. The five stations used for this study are mapped in Figure 3-1 and listed in Table 3-1.

#### 3.1.1 Archival and Extraction of WAVEWATCH III Forecast Data

For each location, the directional wave spectra forecasts by WAVEWATCH III were archived daily. Note that NOAA/NCEP issues WAVEWATCH III forecasts four times per day (at 0000, 0600, 1200, and 1800 GMT), and maintains only the six most recent forecasts on its Web server before removing the oldest forecast and posting the newest forecast, which makes this a time-critical procedure. Forecast archiving began on March 25, 2007, as follows.

At <ftp://ftp.polar.ncep.noaa.gov/waves/>, forecasts are in folders labeled [yyyymmdd.thhz](#), where [yyyymmdd](#) is the year-month-day and [thhz](#) is the hour of the forecast cycle, based on Greenwich Mean Time (GMT), and the variable [hh](#) can be [00](#), [06](#), [12](#), or [18](#). Note that operational forecasts are posted about 5-1/2 hours after the model run for a given forecast cycle. This means that the last forecast of the day, at 1800 GMT, is posted in the [t18z](#) folder for the current day at about 2330 GMT (1630 PDT).

Automated scripts were developed to locate and download the two types of operational WAVEWATCH III forecast files available for each of the five stations, which are named [enp.xxxxx.spec.gz](#) and [enp.xxxxx.bull](#) where [xxxxxx](#) is the data buoy station number. The [spec.gz](#) files contain forecast directional spectra at 3-hour intervals from 0-hours-ahead (the so-

called “nowcast”) out to 180-hours-ahead (7.5-days-ahead) of the time when each forecast is issued, which represents a total of 61 spectra. Only 21 of these were extracted from the archived files:

- 0-hours-ahead (one spectrum),
- from 6-hours-ahead to 72-hours ahead in 6-hour intervals (twelve spectra)
- from 84-hours-ahead to 168-hours-ahead forecasts in 12-hour intervals (eight spectra)

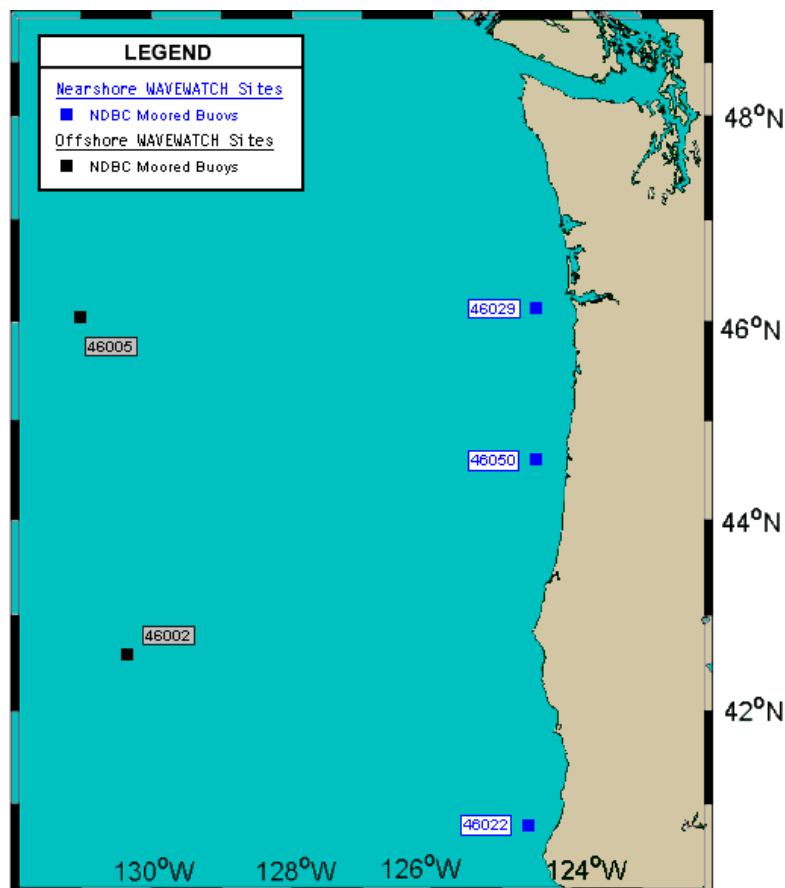


**Figure 3-1.**  
**WAVEWATCH III forecast locations** co-located with NDBC wave measurement stations (offshore = black squares, coastal = blue squares), which were used in this analysis.



**Table 3-1.**  
**List of Stations for Evaluating WAVEWATCH III Forecast Skill**

| Station Number | Agency | Station Description                            | Local Depth | Latitude, Longitude |
|----------------|--------|--|-------------|---------------------|
| 46005          | NDBC   | WASHINGTON - 315n.mi West of Aberdeen, WA      | 2780 m      | 46.05 N, 131.02 W   |
| 46002          | NDBC   | OREGON – 275 n.mi West of Coos Bay, OR         | 3374 m      | 42.6 N, 130.27 W    |
| 46029          | NDBC   | Columbia R. Bar - 78 n.mi S-SW of Aberdeen, WA | 128 m       | 46.12 N, 124.51 W   |
| 46050          | NDBC   | Stonewall Banks, 20 n.mi west of Newport, OR   | 130 m       | 44.62 N, 124.53 W   |
| 46022          | NDBC   | Eel River - 17 n.mi W-SW of Eureka, CA         | 509 m       | 40.78 N, 124.54 W   |

### 3.1.2 Analysis of WAVEWATCH III Forecast Data

The operational WAVEWATCH III directional spectra files contain forecasts at 3-hour intervals from 0-hours-ahead out to 180-hours-ahead (7.5-days-ahead) of the time when each forecast is issued, which represents a total of 61 spectra. Only 21 of these were extracted from the archived files for subsequent analysis, as follows:

- 0-hours-ahead (the so-called “nowcast”) (one spectrum),
- from 6-hours-ahead to 72-hours ahead in 6-hour intervals (twelve spectra)
- from 84-hours-ahead to 168-hours-ahead forecasts in 12-hour intervals (eight spectra)

The directional spectra were reduced to their non-directional form by integrating the directional spectra across all directions. Each non-directional spectrum was then analyzed to yield the following parameters:

- Wave energy flux (watts per meter’s width of a vertical plane intersecting the sea surface; also known as “wave power density”)
- Significant wave height (average of the highest one-third waves)
- Dominant wave period (inverse of frequency at the highest peak in the wave spectrum)
- Wave energy period (average period weighted according to the energy content of each harmonic component in the wave spectrum)

The detailed procedure for reducing directional spectra to non-directional spectra, as well as the equations for calculating each of the above parameters from the non-directional spectrum, are included as Appendix B to this report.

### 3.1.3 Archival of Measured Wave Data

Wave spectra are available at hourly intervals for both the NDBC and CDIP stations listed in Table 2-1. Note, however, that for the NDBC stations, only the raw spectral wave data were available to cover the time period for which we had archived forecasts. Under “Real Time Data” the raw spectral data are only available for the most recent 45 days, whereas under “Historical Data” the quality controlled spectral data are only available with a time lag of two months. This creates a gap of about six weeks for which wave spectra are not posted on the NDBC Web site.

### 3.1.4 Analysis of Measured Wave Data

Unlike the forecast directional wave spectra, the measured wave spectral data are available directly in non-directional form. The same four parameters as listed in Section 3.1.2, above, were calculated from these non-directional spectra, and Appendix B describes the equations used.

### 3.1.5 Time Synchronization of Forecast and Measured Wave Data

The time-series files of calculated parameters were carefully synchronized between the forecasts at different time-ahead horizons and the measured data. Thus, for example, the forecast time series file that begins with the 36-hour-ahead forecast issued at 0000 GMT on 01 May 2007 had to be paired with a measured time series file that begins at 1200 GMT on 02 May 2007.

Figure 3-2, below, gives examples of these synchronized files for wave energy flux at two different forecast time horizons (48-hour-ahead and 168-hour-ahead) for NDBC Station 46002 during June 2007. The deterioration of forecast skill from 48 hours (2 days) ahead to 168 hours (7 days) ahead is clearly evident.

### 3.1.6 Comparison of Forecast and Measured Wave Data

The time-synchronized time series files of measured and forecast sea state parameters for the two far offshore stations (46002 and 46005) and the three near-shore stations (46029, 46050, and 46022) were then subjected to an error analysis, calculating the absolute value of the difference between each measured value and forecast value. These absolute values were averaged to calculate the mean absolute error (MAE) associated with a given forecast time horizon.

Note that MAE values are generally lower than root mean square error (RMSE) values, because the MAE weighs all errors equally, whereas the RMSE gives greater weight to larger errors. Although the RMSE is often used as a metric for judging forecast performance, we chose MAE, because it is associated with the first moment of the prediction error and is thus directly related to energy production potential, whereas RMSE is associated with the second moment and hence to the variance of the prediction error (Reference 7).

Because we anticipate that neural network algorithms might be used to assimilate the measured data into an adjusted forecast, we also wanted to see how well each forecast at a given time horizon correlated with the wave measurement made at that same time. To this end, we performed a standard regression analysis to derive a linear equation that expressed the measured

value of a sea state parameter as a function of its forecast value. We calculated the correlation coefficient from this analysis as the square root of the linear regression r-squared value. This “adjusted forecast” thus corrects for the observed systematic bias in the WAVEWATCH III forecast model.

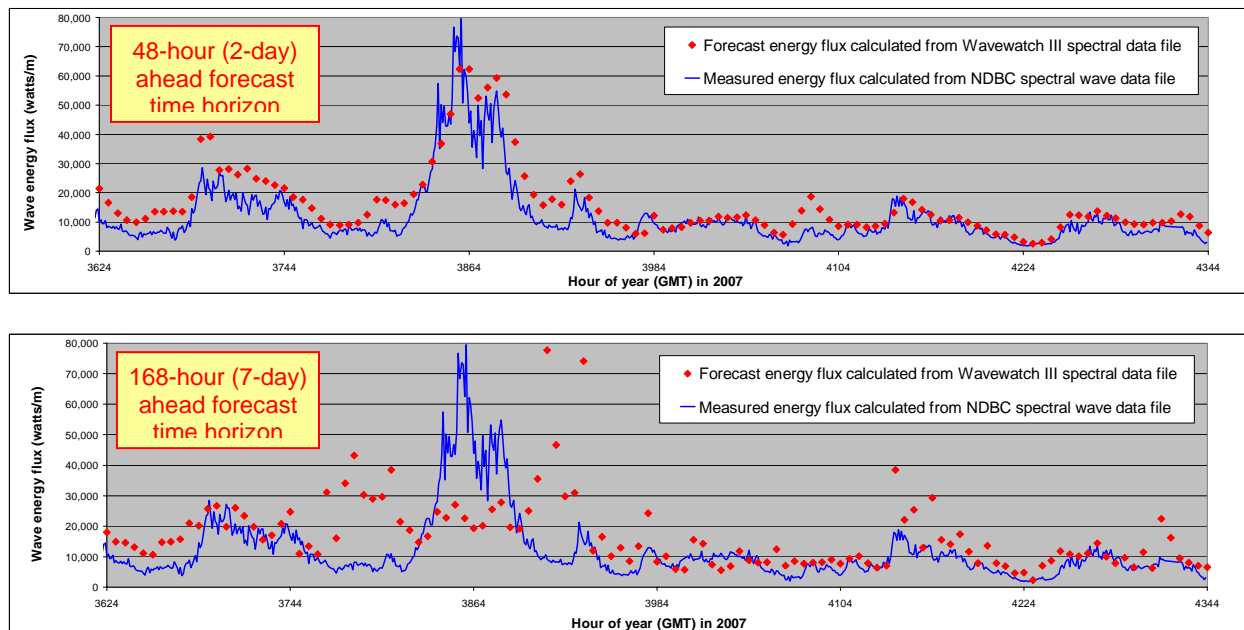


**Figure 3-2.**

### **Comparison of WAVEWATCH III forecast and measured wave energy flux**

At NDBC Station 46002 during the month of June 2007 for two different forecast horizons. The upper graph is for the 48-hour (2-day)-ahead forecast; the lower graph is for the 168-hour (7-day)-ahead forecast. The hour marks on the horizontal axis indicate 5-day intervals.

## **3.2. Correlation of Offshore and Coastal Wave Measurements**

The second major analysis was to characterize the correlation of measured sea state parameters between offshore and coastal data buoy stations, to see if these can be used to “extend the reach” of WAVEWATCH III to locations where its spectral forecast products are not available. For this analysis, we used a year’s worth of NDBC sea state parameters measured at the three stations mapped in Figure 3-3 and listed in Table 3-2.

The first step in determining the correlation between waves at the offshore wave measurement stations and the coastal station was to estimate the time difference or time lag from when a wave train arrives at an offshore buoy to when that same wave train reaches the coastal buoy. For this calculation, wave trains were assumed to travel from northwest to southeast. Based on this assumption, the expected time lag was calculated from the great circle distance between the buoys (calculated from their respective coordinates) and the wave train group velocity derived from the average dominant wave period at the offshore station. As illustrated in the sample calculation shown in Figure 3-4, the time lag was calculated by determining the resultant vector of the waves traveling along a great circle route between the two buoys.

This calculation makes three simplifying assumptions. First it assumes a constant mean wave direction from northwest to southeast. Section 4.2 and Figure 4-15 discusses this assumption and shows that all buoy pairs showed maximum correlation near the predicted time difference assuming a northwest to southeast wave direction. Second, the yearly average dominant wave period is used to calculate the travel time lag, which does not take into account day to day fluctuations in dominant wave period throughout the year. Finally, a constant multiplier of 0.42 is used to calculate wave energy flux, which is more accurately calculated directly from the wave spectrum rather than sea state parameters. Even so, our results for this simplified analysis, presented in Section 4.2, suggest that a more precise analysis (that accounts for variations in dominant wave period, mean wave direction, and spectral shape) is unlikely to lead to a different conclusion.

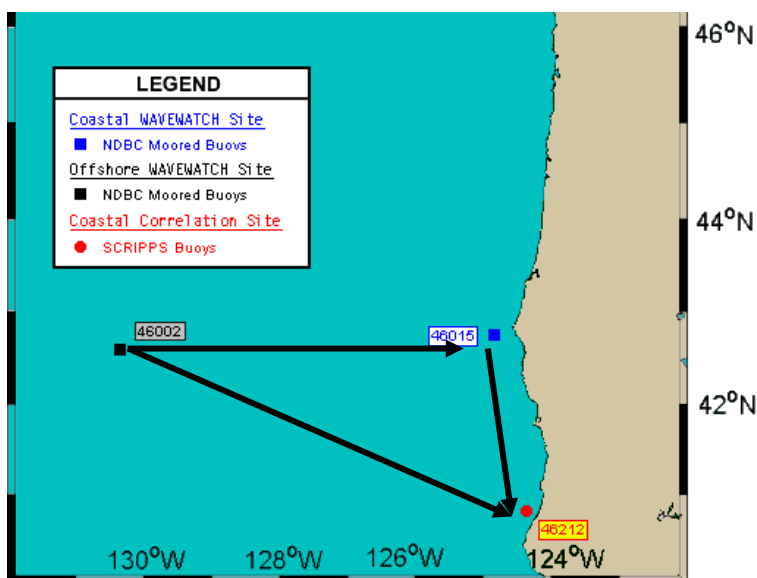


**Figure 3-3.**

**NDBC and CDIP wave measurement stations used in this analysis.**

Arrows indicate sense of correlation from offshore to coastal; all wave trains are assumed to travel from northwest to southeast, which is the predominant direction of swells emanating from winter storms in the Gulf of Alaska. Although swell trains coming from the southwest are occasionally present from storms in the Southern Ocean, these have much lower energy content because these storms are so much farther away.

**Table 3-2.**

**List of Stations for Correlating Offshore and Coastal Wave Measurements**

| Station Number | Agency | Station Description                           | Local Depth | Latitude, Longitude |
|----------------|--------|---|-------------|---------------------|
| 46002          | NDBC   | OREGON – 275 n.mi West of Coos Bay, OR        | 3374 m      | 42.6 N, 130.27 W    |
| 46015          | NDBC   | Port Orford - 16 n.mi West of Port Orford, OR | 448 m       | 42.75 N 124.85W     |
| 46212          | CDIP   | Humboldt Bay South Spit, CA (128)             | 40 m        | 40.75 N 124.31 W    |

Standard Meteorological Data from the 2006 calendar year were downloaded from the NDBC Web site (<http://www.ndbc.noaa.gov/>), which were available in the form of raw text files viewable online at [http://www.ndbc.noaa.gov/historical\\_data.shtml#stdmet](http://www.ndbc.noaa.gov/historical_data.shtml#stdmet). Two specific data columns from the data sets, significant wave height (WVHT) and dominant wave period (DPD), were used to calculate wave energy flux (J) according to the following equation:

$$P = .42(WVHT^2)(DPD)$$

#### Time Lag Calculation

Offshore Buoy: 46015

Location: Port Orford

Latitude, Longitude: 42°45'24" N, 124°49'45" W

Coastal Buoy: 46212

Location: Humboldt Bay, South Spit

Latitude, Longitude: 40°45'12" N, 124°18'48" W

Distance = 140.927 mi

Horizontal Distance = 26.166 mi

Average Dominant Wave Period (DPD): 11.925s

$$\text{Wave Length} = \frac{9.8(DPD^2)}{6.28} = 221.913m$$

Wave Speed = Wave Length / DPD = 18.609 m/s

Energy Speed = Wave Speed / 2 = 9.305 m/s = 20.814 mph

$$b = \sin^{-1}\left(\frac{26.166}{140.927}\right)$$

$$a = 45 - b$$

$$d = 140.927 \cos(a)$$

$$\text{time} = d / \text{Energy Speed} = 5.6 \text{ hrs}$$

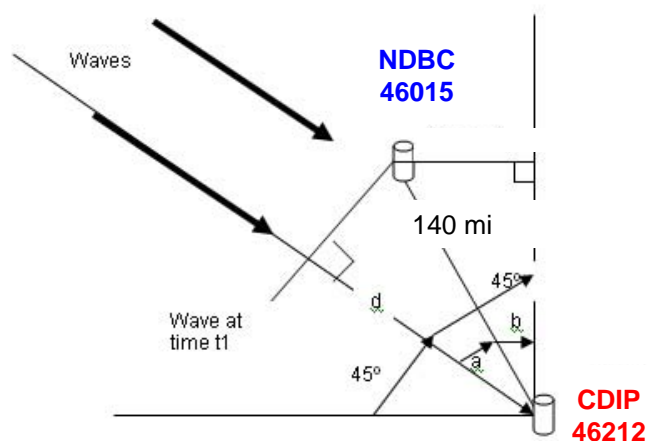


**Figure 3-4.**  
**Example of travel time calculation for offshore wave train.**

### 3.3. Influence of Sea vs. Swell Dominance on Measurement Correlations

To see how well wave measurements were correlated up and down the coast in different types of sea states, we performed a series of pair-wise regression analyses between three near-shore NDBC stations where WAVEWATCH III forecast products are available and three coastal measurement stations where such forecasts are not available (see Figure 3-5 and Table 3-3).

These correlations were done for subsets of time series data points that could be identified clearly as “sea events” (increase in significant wave height accompanied by gradual rise in peak wave period) and as “swell events” (increase in significant wave height accompanied by abrupt jump in peak wave period followed by gradual decrease in peak period).

Note that this series of swell analyses does not make any assumption about directionality or group velocity of the prevailing swell but simply iterates through a realistic range of time lags and selects the time lag that yields the highest correlation coefficient for a particular event and buoy pair. This type of analysis lends itself well to neural network “learning” such that evolving “correlation rules” could be developed in an actual operational forecasting model.

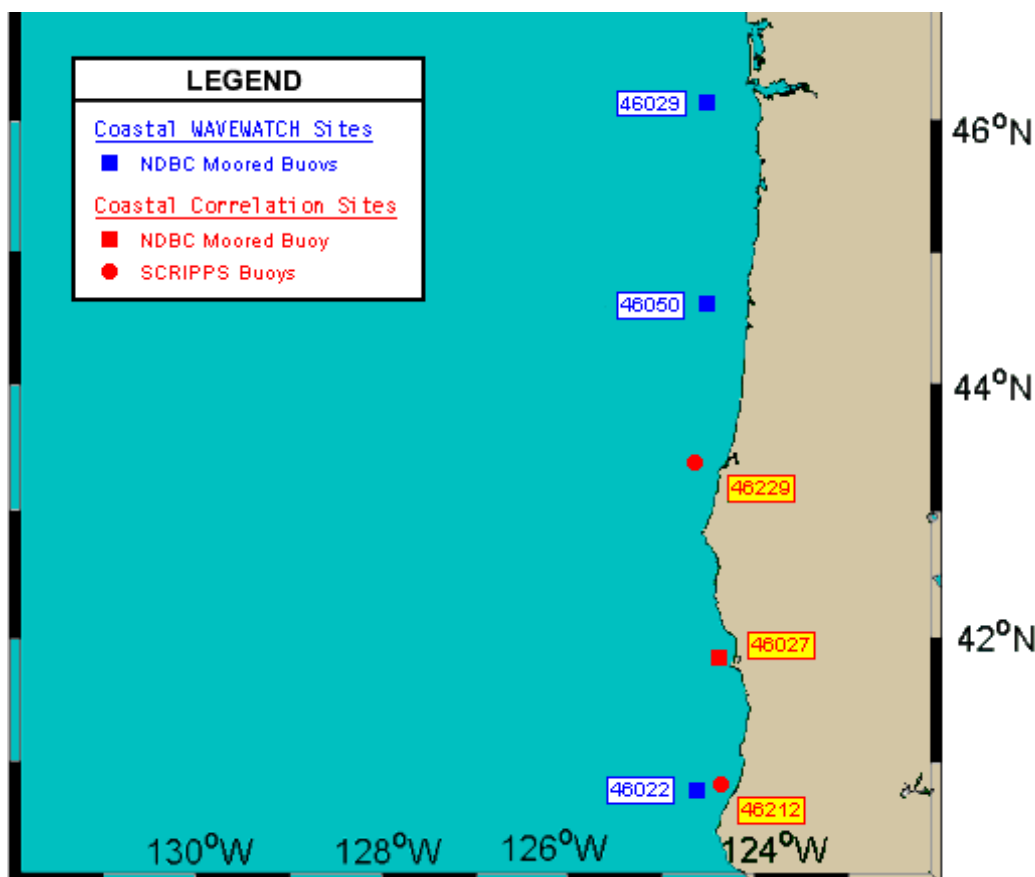


**Figure 3-5.**  
NDBC and CDIP wave measurement stations used in this analysis.

**Table 3-3.****List of Stations for Evaluating Sea State Influence on Coastal Correlations**

| Station Number | Agency | Station Description                            | Local Depth | Latitude, Longitude |
|----------------|--------|--|-------------|---------------------|
| 46029          | NDBC   | Columbia R. Bar - 78 n.mi S-SW of Aberdeen, WA | 128 m       | 46.12 N 124.51 W    |
| 46050          | NDBC   | Stonewall Banks, 20n.mi west of Newport, OR    | 130 m       | 44.62°N, 124.53°W   |
| 46022          | NDBC   | Eel River - 17 n.mi W-SW of Eureka, CA         | 509 m       | 40.78 N 124.54 W    |
| 46229          | CDIP   | Umpqua Offshore, OR (139)                      | 187 m       | 43.77°N, 124.55°W   |
| 46027          | NDBC   | St Georges - 8 n.mi W-NW of Crescent City, CA  | 48 m        | 41.85 N 124.38 W    |
| 46212          | CDIP   | Humboldt Bay South Spit, CA (128)              | 40 m        | 40.75 N 124.31 W    |





# 4

## RESULTS

### 4.1. Evaluation of WaveWatch III Forecast Skill

Figures 4-1 through 4-6 plot the mean absolute error (MAE) for all four sea state parameters at the northernmost far offshore station (46005) and the northernmost near-shore station (46029). The patterns and trends shown in these figures are very similar for the other three stations (offshore: 46002, and near-shore: 46050, and 46022). For the sake of brevity those plots are omitted here but are included in Appendix C of this report, which presents measurement and forecast comparison plots for all four sea state parameters at all five stations.

To enable ready comparison between the offshore and near-shore buoys for each parameter, the plots of MAE are presented in the following order on the next three pages: wave energy flux in Figures 4-1 and 4-2, significant wave height in Figures 4-3 and 4-4, and the two wave period parameters in Figures 4-5 and 4-6. Results from the far offshore station 46005 are presented at the top of each page, while those for near-shore station 46029 are presented at the bottom.

The following trends are evident in our results:

- (A) The MAE in wave energy flux and significant wave height at a given station follow the same trend, which is to be expected, given that wave energy flux is proportional to the square of significant wave height.
- (B) The wave energy flux and significant wave height forecasts at the far offshore station show relatively constant accuracy out to 24 hours ahead, at which point the MAE begins to rise gradually, being 50% greater at 72 hours ahead and then leveling off again. Beyond 5.5-days ahead, these forecasts deteriorate rapidly.
- (C) The wave energy flux and significant wave height forecasts at the near-shore station show the same pattern, except that the early constant forecast accuracy holds a bit longer, almost out to 48 hours ahead before rising significantly.
- (D) At all forecast horizons, the forecast of wave energy period ( $T_e$ ) is much better than the forecast for dominant period ( $T_p$ ), which is to be expected, because  $T_e$  is derived from the shape of the full spectrum, whereas  $T_p$  is based on only the highest peak in the spectrum. In the multi-peaked spectra that are common off the Pacific Northwest, WAVEWATCH III can be quite accurate at forecasting the spectral shape, but if one of its forecast peaks is only slightly higher than the measured spectral peak at another frequency, then there will be a large error in  $T_p$ .
- (E) The forecast accuracy for both period parameters is relatively constant out to 72 hours ahead, when it begins rising significantly, deteriorating more rapidly at the far offshore station than the near-shore station.

- (F) At all forecast horizons and for all four sea state parameters, the original forecast is more accurate at the near-shore station than at the far offshore station
- (G) At all forecast horizons and for all four sea state parameters, the far offshore station shows much greater improvement in the adjusted forecast over the original forecast, with the overall result that the adjusted forecast errors are more similar between the two stations. Even so, however, the final adjusted forecasts for  $H_s$ ,  $T_e$ , and  $T_p$  are still somewhat better at the near-shore stations than at the far offshore stations.

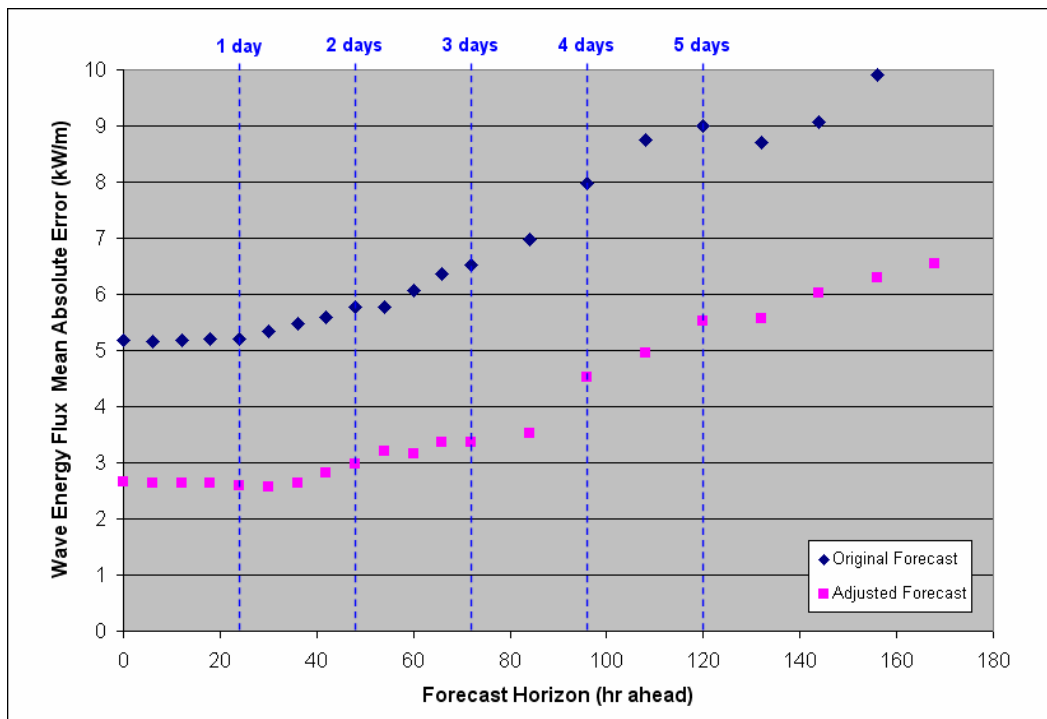


**Figure 4-1.**

**Mean absolute error of WAVEWATCH III forecast for wave energy flux at far offshore NDBC Station 46005 during the period from 24 May through 30 September 2007.**

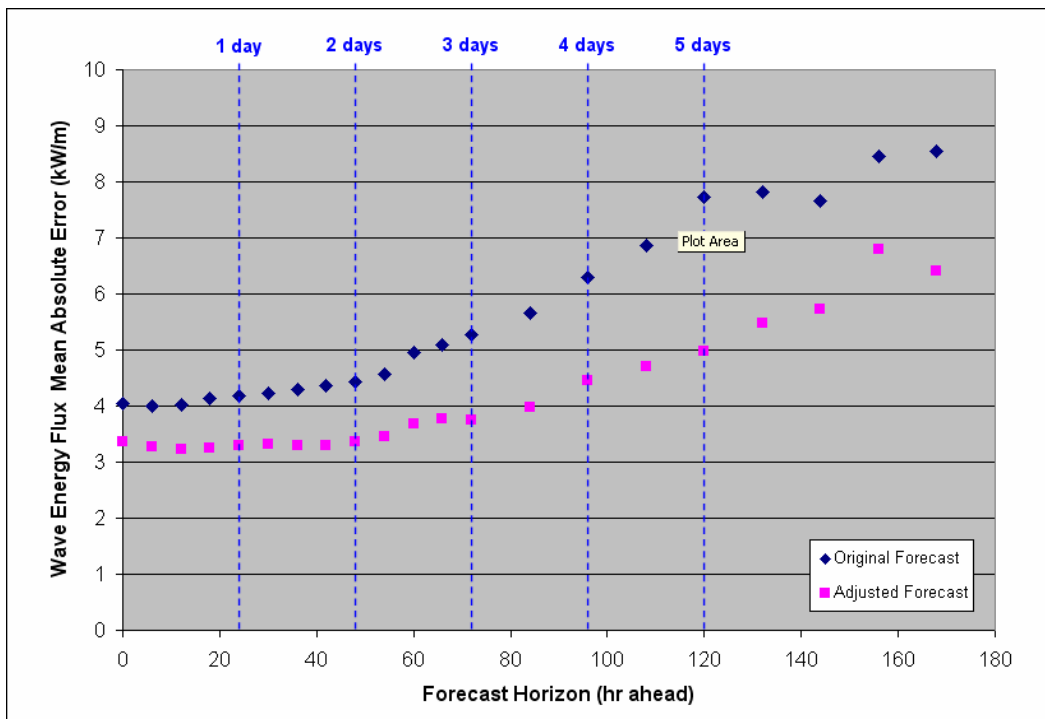


**Figure 4-2.**

**Mean absolute error of WAVEWATCH III forecast for wave energy flux at near-shore NDBC Station 46029 during the period from 24 May through 30 September 2007.**

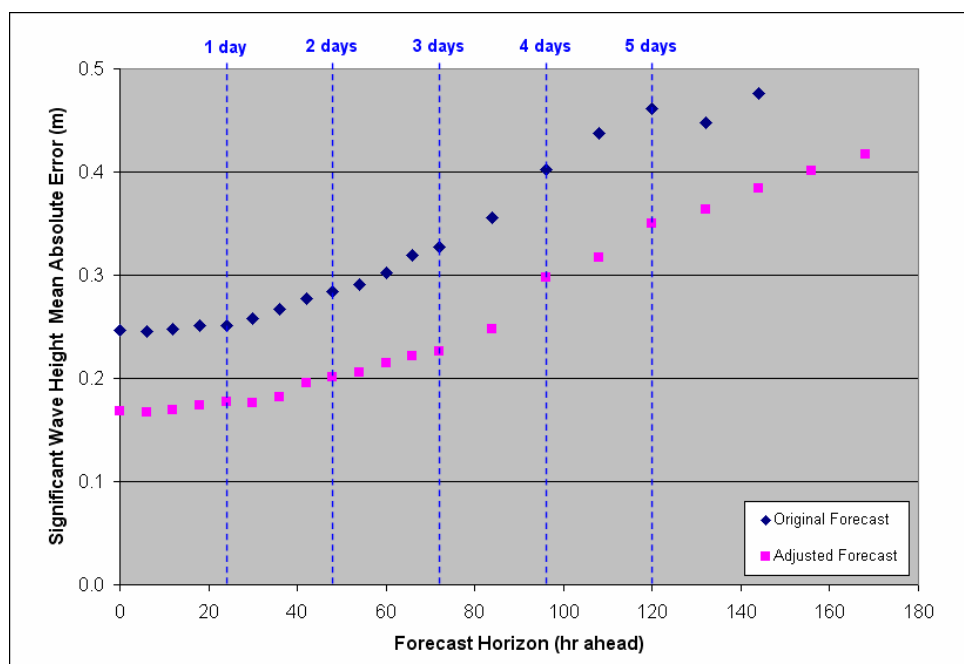


**Figure 4-3.**

**Mean absolute error of WAVEWATCH III forecast for significant wave height at far offshore NDBC Station 46005 during the period from 24 May through 30 September 2007.**

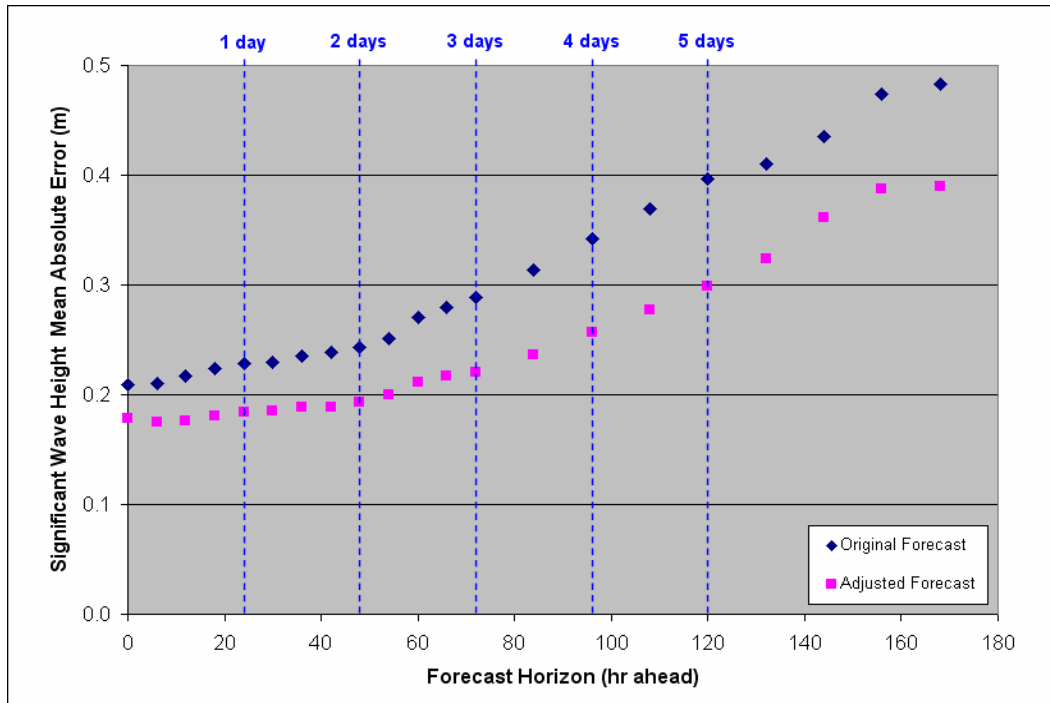


**Figure 4-4.**  
Mean absolute error of WAVEWATCH III forecast for significant wave height at near-shore NDBC Station 46029 during the period from 24 May through 30 September 2007.

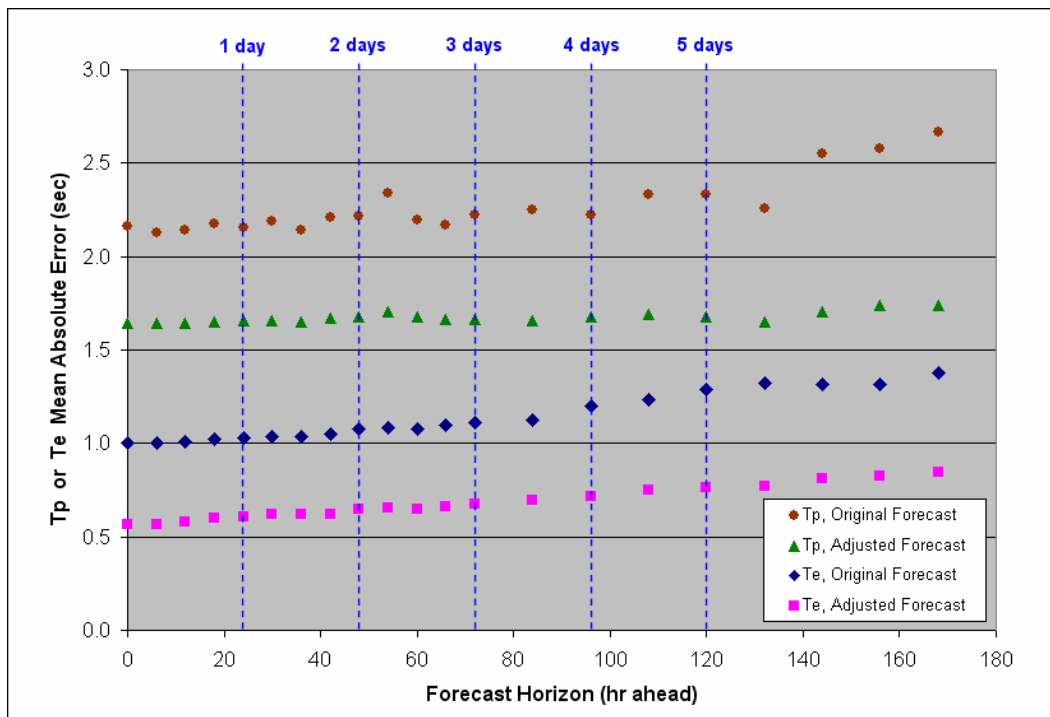


**Figure 4-5.**  
Mean absolute error of WAVEWATCH III forecast for two wave period parameters at far offshore NDBC Station 46005 during the period from 24 May through 30 September 2007.

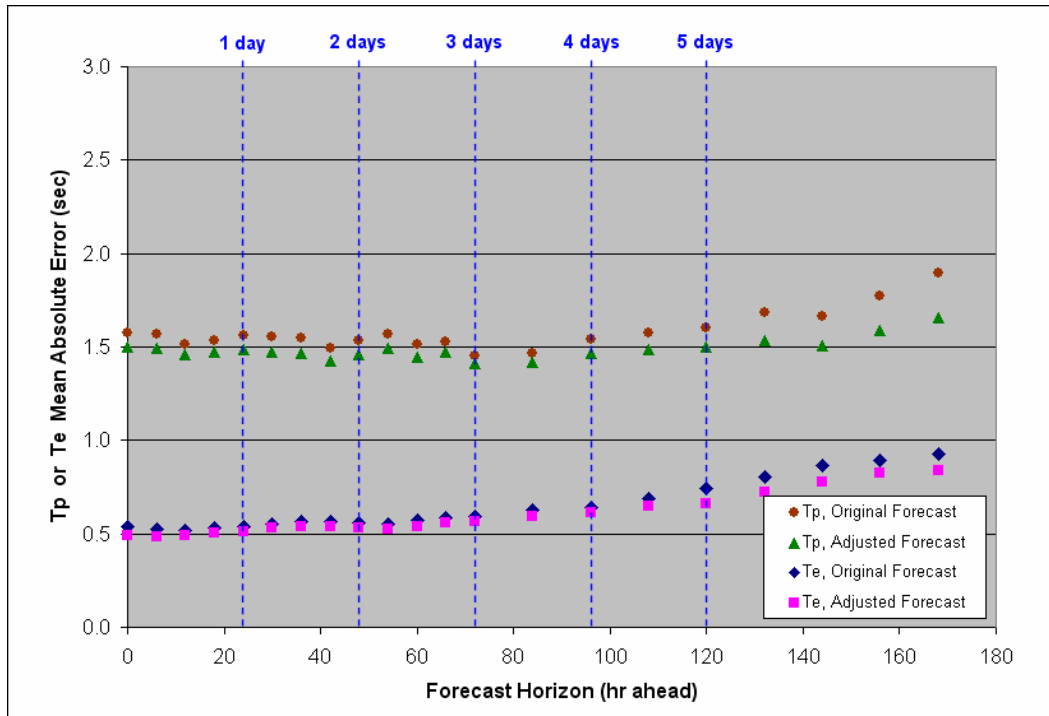


**Figure 4-6.**

**Mean absolute error of WAVEWATCH III forecast for two wave period parameters at near-shore NDBC Station 46029 during the period from 24 May through 30 September 2007.**

Recalling from the introduction (Section 1.2) that 48-hours is the forecast time horizon at which accurate estimates of significant wave height ( $H_s$ ; to within  $\pm 0.25$  m) and wave energy period ( $T_e$ ; to within  $\pm 1.0$  sec) are required in order to yield useful data about future wave power plant performance to control area dispatchers, the following tables summarize our results from all five co-located WAVEWATCH III forecast output stations and measurement buoy stations, covering the forecast dates from 24 May through 30 September 2007.

**Table 4-1.**

**WAVEWATCH III Original Forecast Skill at 48 Hours Ahead**

| Station Number | Station Description                            | Local Depth | Mean Absolute Error |             |
|----------------|--|-------------|---------------------|-------------|
|                |  |             | $H_s$ (m)           | $T_e$ (sec) |
| 46005          | WASHINGTON - 315n.mi West of Aberdeen, WA      | 2780 m      | 0.28                | 1.08        |
| 46002          | OREGON – 275 n.mi West of Coos Bay, OR         | 3374 m      | 0.29                | 1.34        |
| 46029          | Columbia R. Bar - 78 n.mi S-SW of Aberdeen, WA | 128 m       | 0.24                | 0.56        |
| 46050          | Stonewall Banks, 20 n.mi west of Newport, OR   | 130 m       | 0.24                | 1.04        |
| 46022          | Eel River - 17 n.mi W-SW of Eureka, CA         | 509 m       | 0.38                | 0.62        |

**Table 4-2.**  
**WAVEWATCH III Adjusted Forecast Skill at 48 Hours Ahead**

| Station Number | Station Description                            | Local Depth | Mean Absolute Error |          |
|----------------|--|-------------|---------------------|----------|
|                |  |             | Hs (m)              | Te (sec) |
| 46005          | WASHINGTON - 315n.mi West of Aberdeen, WA      | 2780 m      | 0.20                | 0.65     |
| 46002          | OREGON – 275 n.mi West of Coos Bay, OR         | 3374 m      | 0.26                | 0.74     |
| 46029          | Columbia R. Bar - 78 n.mi S-SW of Aberdeen, WA | 128 m       | 0.19                | 0.53     |
| 46050          | Stonewall Banks, 20 n.mi west of Newport, OR   | 130 m       | 0.21                | 0.79     |
| 46022          | Eel River - 17 n.mi W-SW of Eureka, CA         | 509 m       | 0.26                | 0.60     |

The adjusted forecast appears to largely meet our required accuracy criterion for significant wave height at all five stations, ranging from +/- 0.19 m to +/-0.26 m, not quite meeting the criterion at two out of five stations. Adjusted forecast skill for wave energy period meets our criterion, with adjusted forecast errors ranging from +/- 0.53 sec to +/- 0.79 sec. The adjusted forecast accuracy is therefore very nearly as good as (for Hs) or better than (for Te) the sea state resolution with which Reference 4 requires wave energy device developers to specify their power output.

One of the most striking results of our analysis is the difference between the far offshore buoys and near-shore buoys in the degree of correlation between WAVEWATCH III forecasts and buoy measurements. These correlations are plotted in Figures 4-9 and 4-10 for the two far offshore buoys (46002 and 46005), and in Figures 4-11 through 4-13 for the three near-shore buoys (46022, 46029, and 46050).

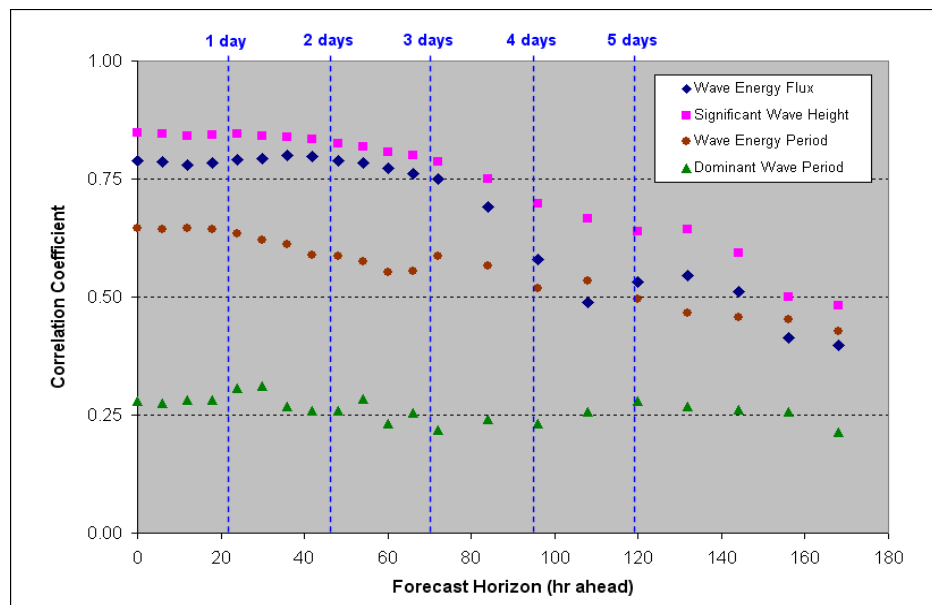


**Figure 4-9.**  
**Correlation between measured and forecast sea state parameters at far offshore NDBC Station 46002 during the period from 24 May through 30 September 2007.**

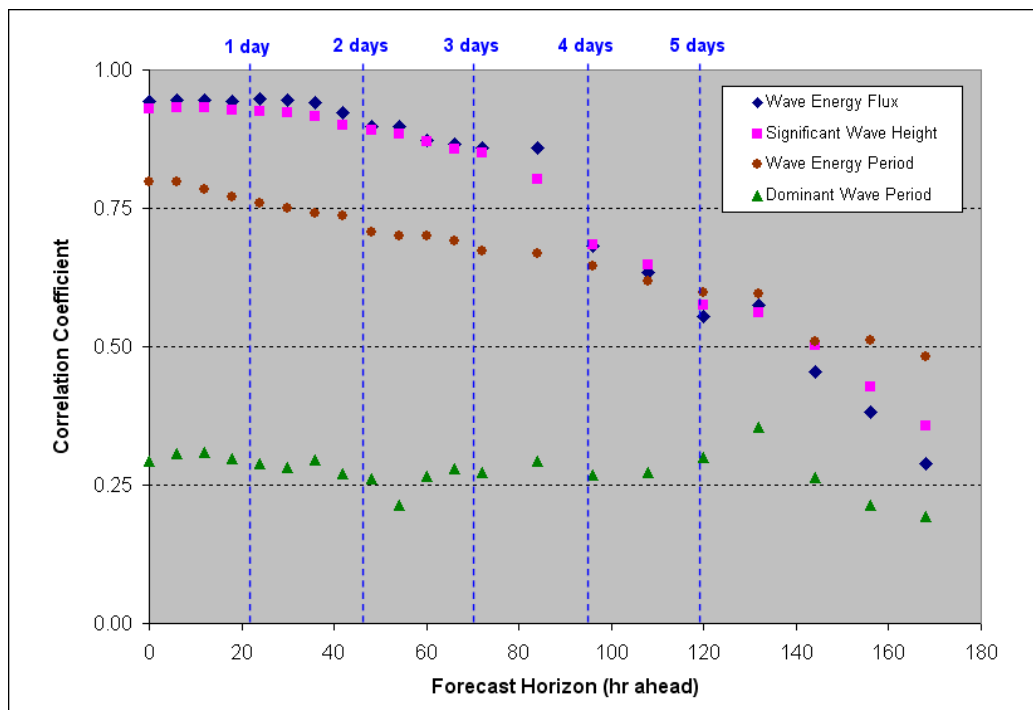


**Figure 4-10.**  
Correlation between measured and forecast sea state parameters at far offshore NDBC Station 46005 during the period from 24 May through 30 September 2007.

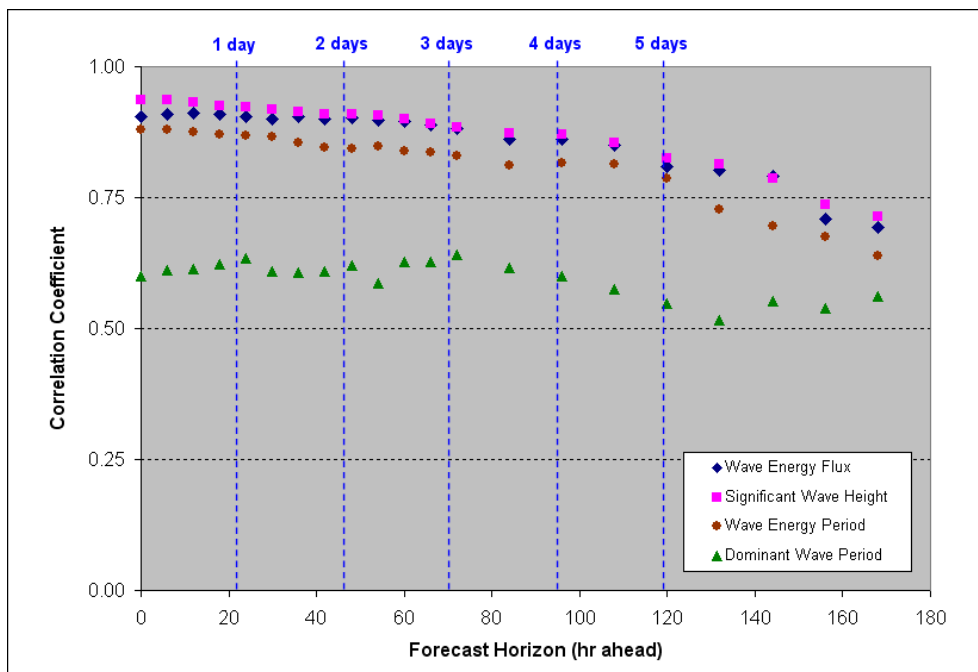


**Figure 4-11.**  
Correlation between measured and forecast sea state parameters at near-shore NDBC Station 46022 during the period from 24 May through 30 September 2007.

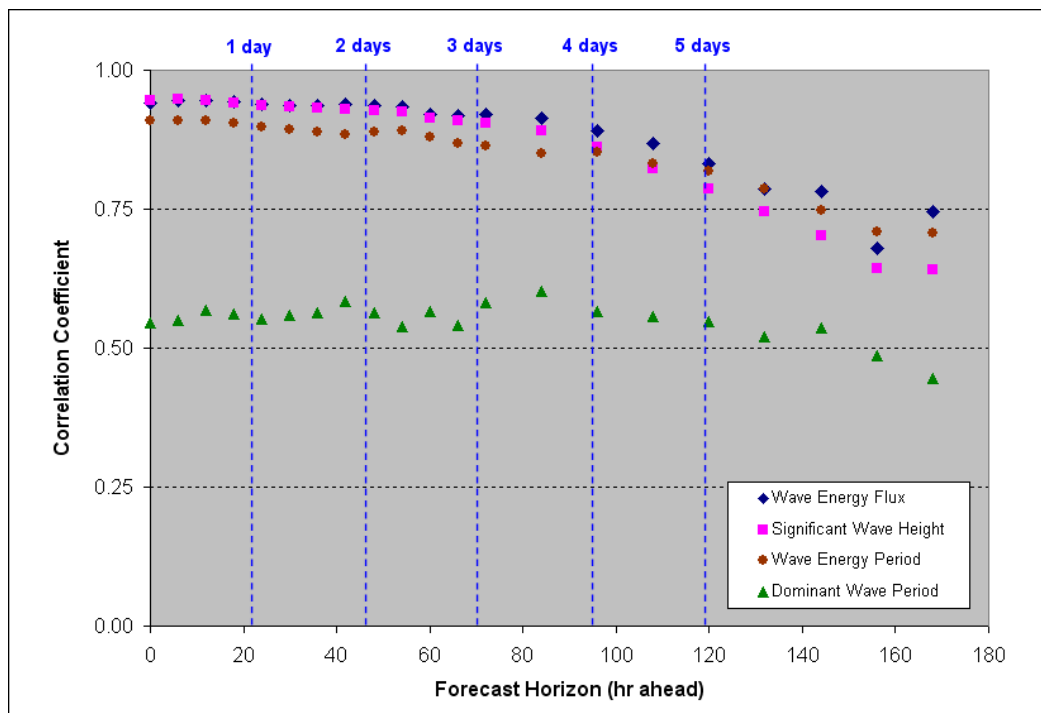


**Figure 4-12.**  
Correlation between measured and forecast sea state parameters at near-shore NDBC Station 46029 during the period from 24 May through 30 September 2007.

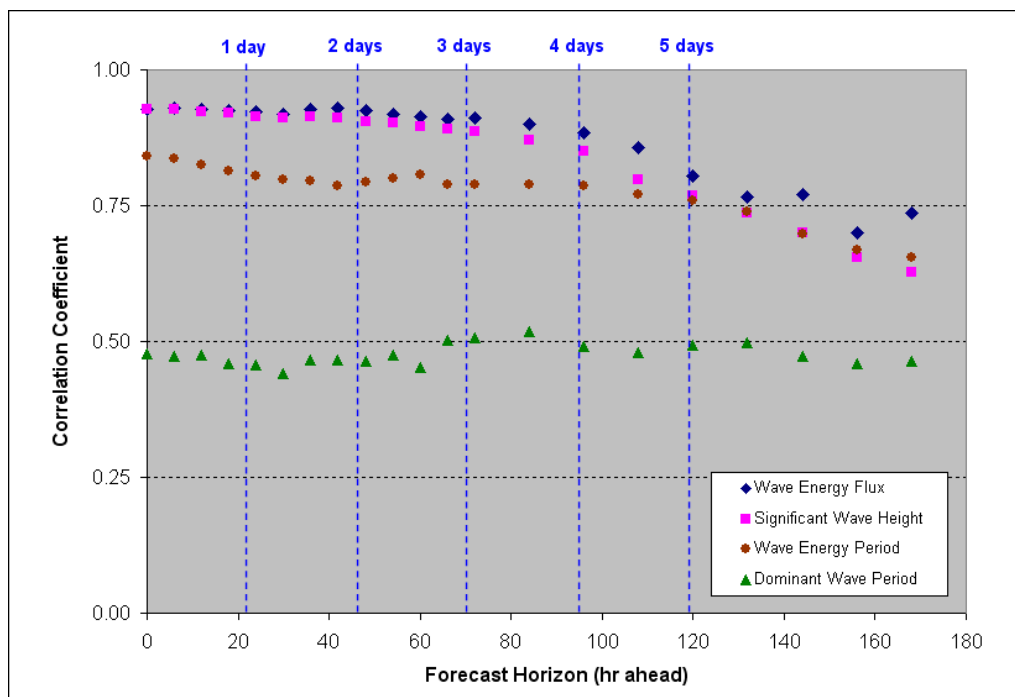


**Figure 4-13.**  
Correlation between measured and forecast sea state parameters at near-shore NDBC Station 46050 during the period from 24 May through 30 September 2007.



At the two far offshore stations, the correlation coefficient for significant wave height drops below 75% at 3 to 4 days ahead, and the correlation coefficient for wave energy period drops below 75% between 1 and 2 days ahead at Station 46005, and is below 65% for all forecast horizons at Station 46002.

By comparison, the correlation coefficient for both sea state parameters is greater than 75% out to 5 days ahead for all three near-shore stations. The 75% correlation coefficient threshold is significant, because Debs et al (Reference 8) found that ANNSTLF forecasts could be improved by learning from measurements (relative to the case of no measurements) only if the correlation coefficient is 75% or higher. This suggests that the accuracy of WAVEWATCH III operational forecasts at routine output locations can be adjusted to exceed our accuracy criteria out to five days ahead by using a neural network engine to adjust future forecasts based on learning from the regression relationship between past forecasts and past measurements. This possibility is conceptually illustrated in Figure 4-14.

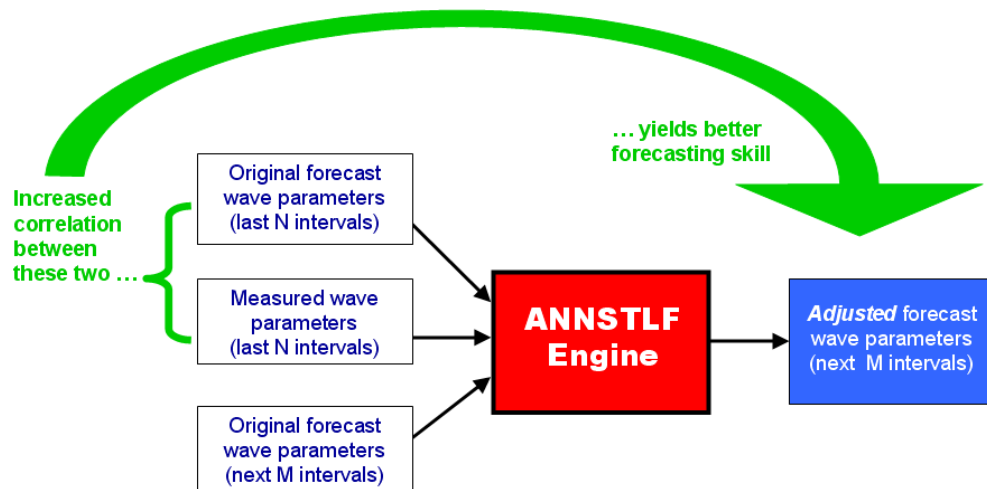


**Figure 4-14.**

**Conceptual diagram showing how good correlation between past original forecasts and past measurements can be used to adjust future WAVEWATCH III forecasts.**

Future studies should be directed at determining the values of N (how many past time intervals should be used to determine the regression relationship) and M (how many future time intervals should have the regression relationship applied to them). Note that 6 hours is the time interval at which WAVEWATCH forecasts are issued. Thus a moving look-back period of three to five days would yield N values ranging from 12 to 20 data points. If the resulting regression relationships are applied to the next day's four forecasts (i.e. at 0000, 0600, 1200, and 1800 GMT), then the value of M is 4.

## 4.2. Correlation of Offshore and Coastal wave Measurements

The goal of this analysis was to evaluate the effect of increased distance between buoys on power density correlation and the time lag corresponding to maximum correlation. Correlation coefficients were calculated for all hourly time lags between 0 and 23 hours, for three pair-wise combinations of the three buoys (refer back to Figure 3-3):

46002 → 46212 (predicted time lag of maximum correlation = 16 hours)

46002 → 46015 (predicted time lag of maximum correlation = 11 hours)

46015 → 46212 (predicted time lag of maximum correlation = 5.6 hours)

As shown below in Figure 4-15, all buoy pairs showed maximum correlation near the predicted time difference (which assumed northwest to southeast wave direction). There is a pronounced decrease in maximum correlation with an increasing distance between the stations. A likely explanation is that over the longer travel distances, wave trains undergo additional dispersion of harmonic components as well as having increased exposure to local wind effects.

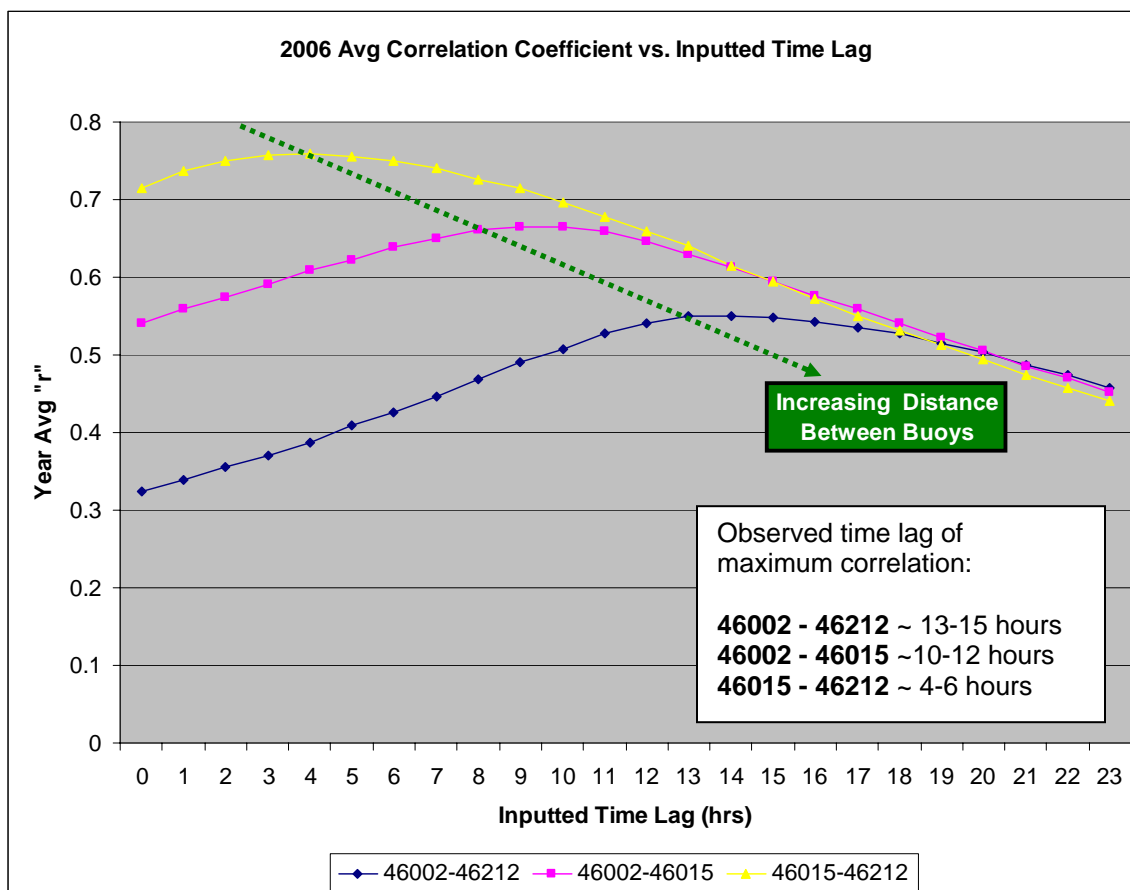


**Figure 4-15.**

Graph of correlation vs. time lag for the three offshore-coastal buoy pairs demonstrates the decreasing maximum correlation with increasing distance between stations. The approximate lag times for maximum observed correlation are also indicated.

The closest buoy pair (46015 – 46212) yielded a maximum correlation coefficient of 76%, while the 46002 – 46015 pair (greater separation distance) exhibited a lower maximum correlation coefficient of 67%, and the farthest-apart pair (46002 – 46212) produced the lowest maximum correlation coefficient of 55%. This analysis suggests that measured wave conditions at far offshore buoys cannot be used with great confidence to forecast wave conditions nearer shore.

Note, however, that correlation was relatively high for the closest buoy pair, exceeding the 75% threshold for successful use of the EPRI ANNSTLF neural network engine. This supports our hypothesis that WAVEWATCH III forecasts at a given near-shore station can be used to predict power density at nearby coastal buoys, as conceptually illustrated in Figure 4-16. The next section explores what distance constitutes a sufficiently “nearby” buoy to make this forecast extrapolation possible, and how it is influenced by type of sea state (sea or swell).

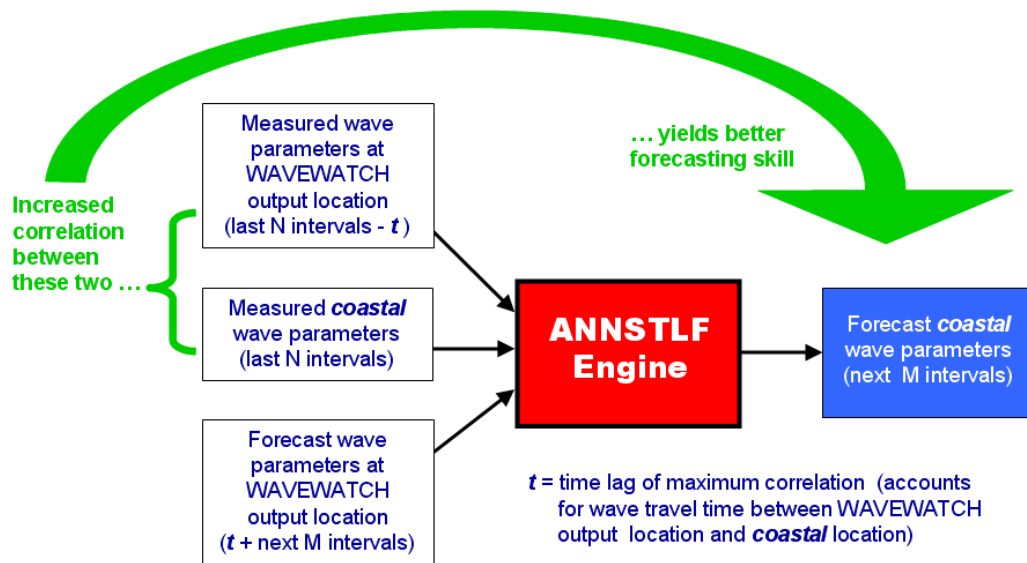


**Figure 4-16.**  
Conceptual diagram showing how well-correlated measurements can be used to extend the reach of near-shore WAVEWATCH III forecasts to nearby coastal buoys.

#### 4.3. Influence of Sea vs Swell Dominance on Coastal Measurement Correlations

To see how closely wave measurements were correlated up and down the coast in different types of sea states, we performed a series of pair-wise regression analyses between three near-shore NDBC stations where WAVEWATCH III forecast output products are available and three coastal measurement stations where such forecasts are not available (refer back to Figure 3-5 and Table 3-3). Because all of these buoys are relatively close to the coast, their great circle separation distances are nearly the same as their north-south latitude separation distances. Note that all of the coastal buoys are north of the southernmost near-shore station (46022), and so these separation distances are assigned a negative value in the following graphs.

Figures 4-17 and 4-18 show the pair-wise correlation of measured wave energy flux as a function of distance between the buoys in a given pair. The correlations for “swell events” are plotted in Figure 4-17, and the correlations for “sea events” are plotted in Figure 4-18.

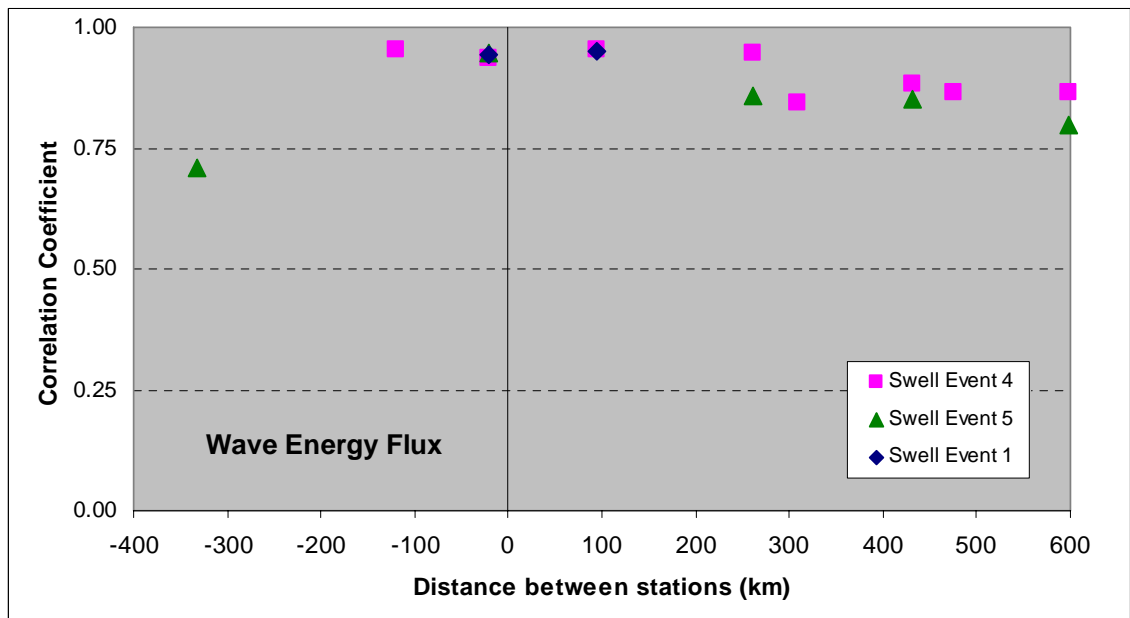


**Figure 4-17.**  
Correlation between measured wave energy flux at pairs of buoys as a function of the distance between buoys for “swell events” in May through September 2007.

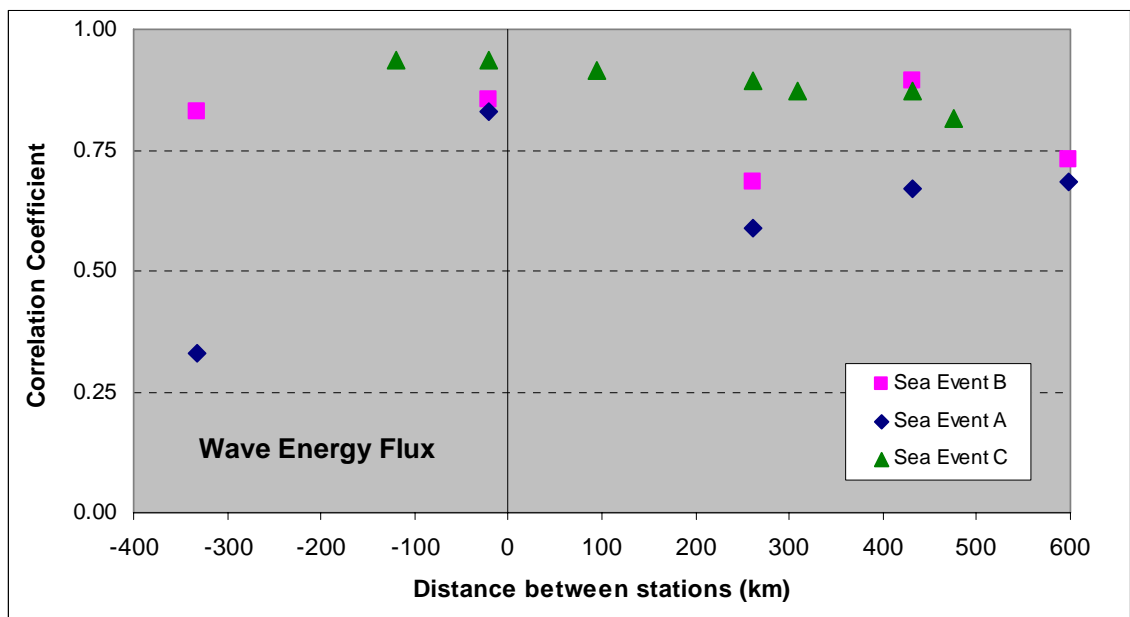


**Figure 4-18.**  
Correlation between measured wave energy flux at pairs of buoys as a function of the distance between buoys for “sea events” in May through September 2007.

Figures 4-19 and 4-20 show the pair-wise correlation of measured significant wave height ( $H_s$ ) as a function of distance between the buoys in a given pair. The correlations for “swell events” are plotted in Figure 4-19, and the correlations for “sea events” are plotted in Figure 4-20.

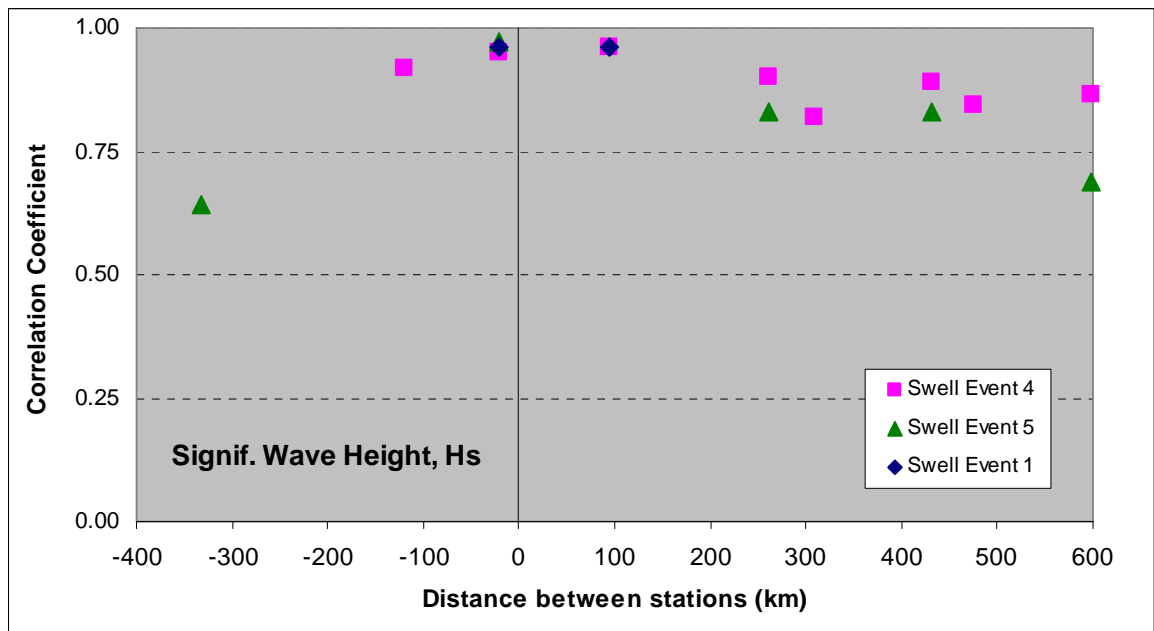


**Figure 4-19.**  
Correlation between measured significant wave height at pairs of buoys as a function of the distance between buoys for “swell events” in May through September 2007.

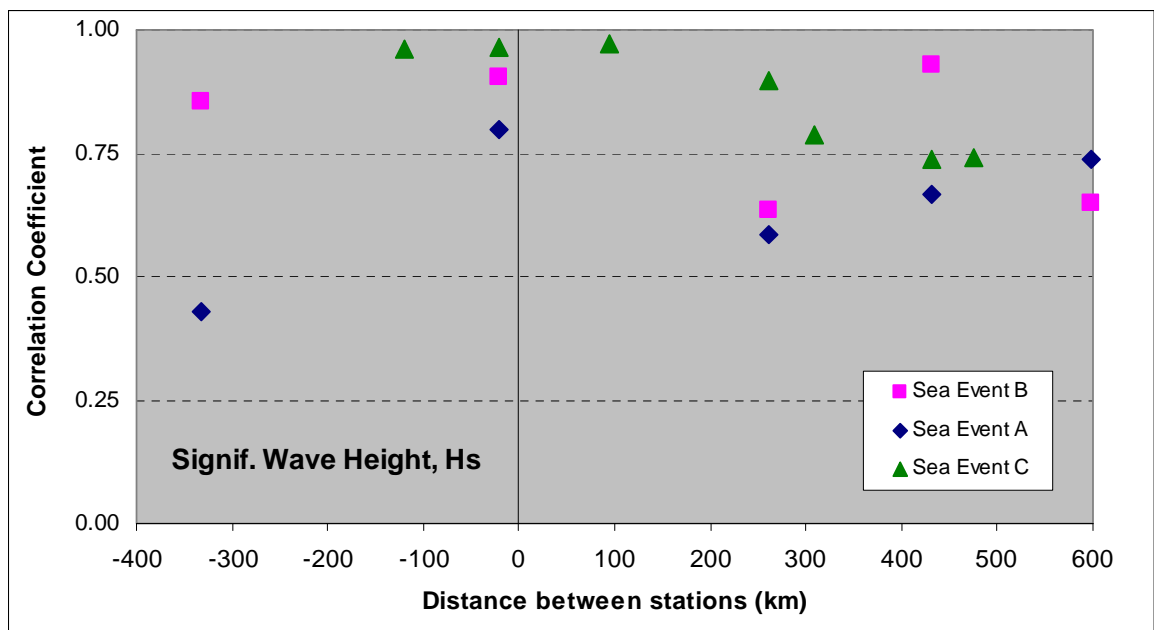


**Figure 4-20.**  
Correlation between measured significant wave height at pairs of buoys as a function of the distance between buoys for “sea events” in May through September 2007.

Figures 4-21 and 4-22 show the pair-wise correlation of measured wave energy period ( $T_e$ ) as a function of distance between the buoys in a given pair. The correlations for “swell events” are plotted in Figure 4-21, and the correlations for “sea events” are plotted in Figure 4-22.

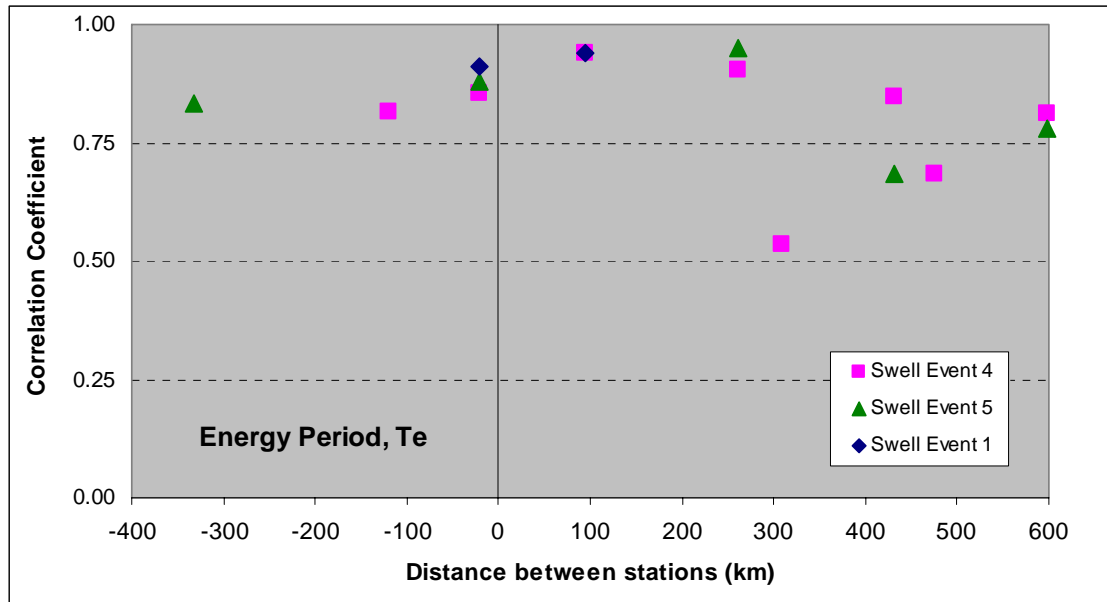


**Figure 4-21.**  
Correlation between measured energy period at pairs of buoys as a function of the distance between buoys for three “swell events” in May through September 2007.

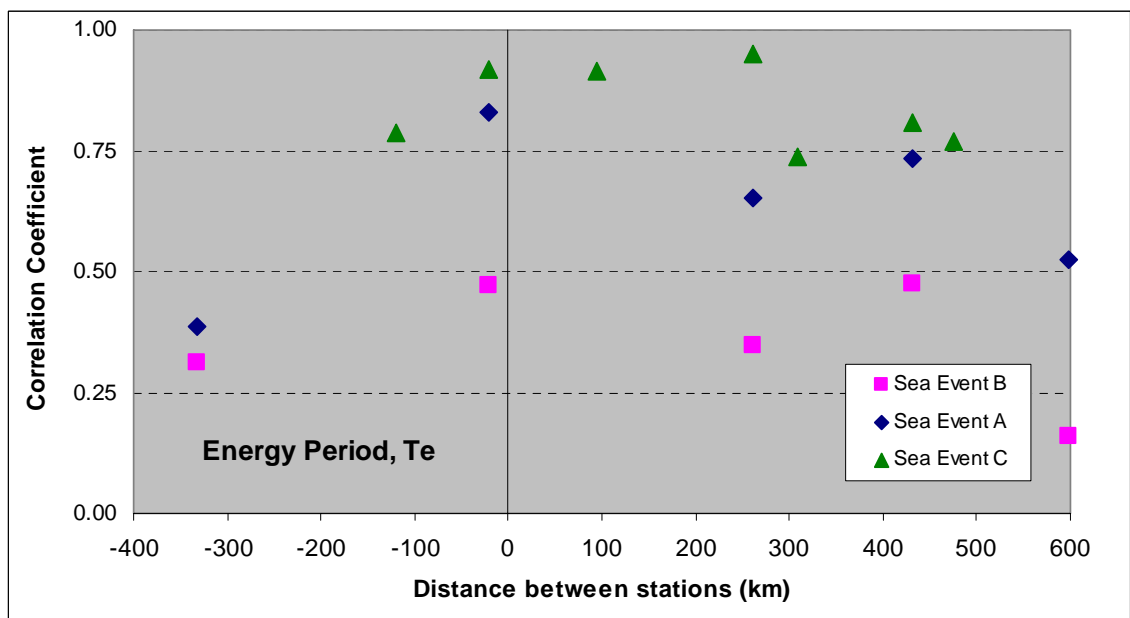


**Figure 4-22.**  
Correlation between measured energy period at pairs of buoys as a function of the distance between buoys for three “sea events” in May through September 2007.

Figures 4-23 and 4-24 show the pair-wise correlation of measured dominant period ( $T_p$ ) as a function of distance between the buoys in a given pair. The correlations for “swell events” are plotted in Figure 4-23, and the correlations for “sea events” are plotted in Figure 4-24.

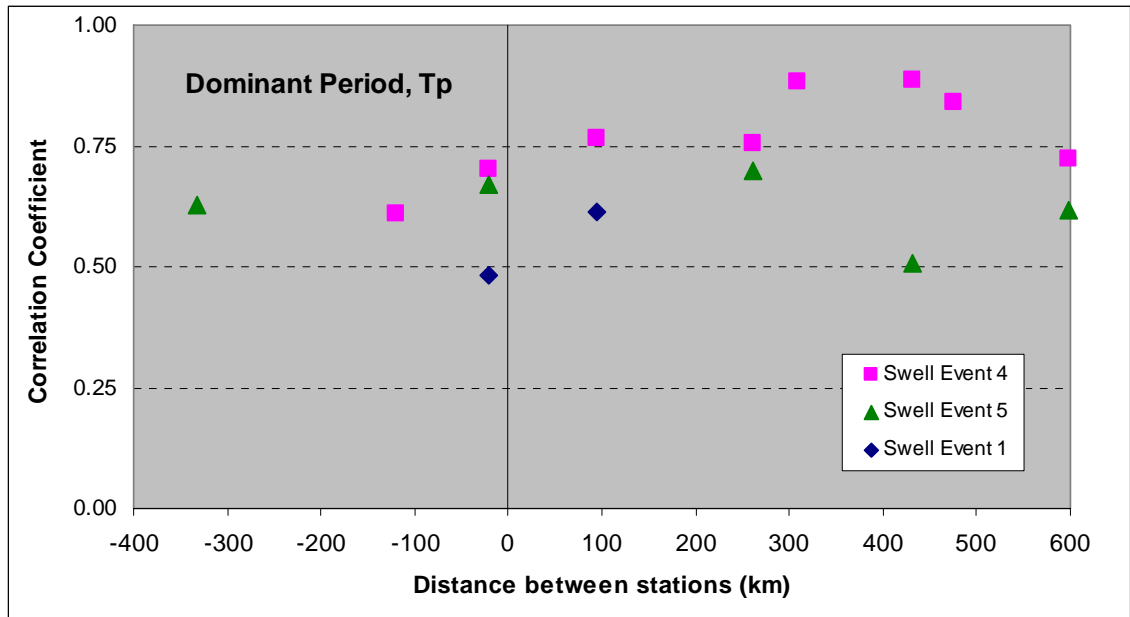


**Figure 4-23.**  
Correlation between measured dominant period at pairs of buoys as a function of the distance between buoys for three “swell events” in May through September 2007.

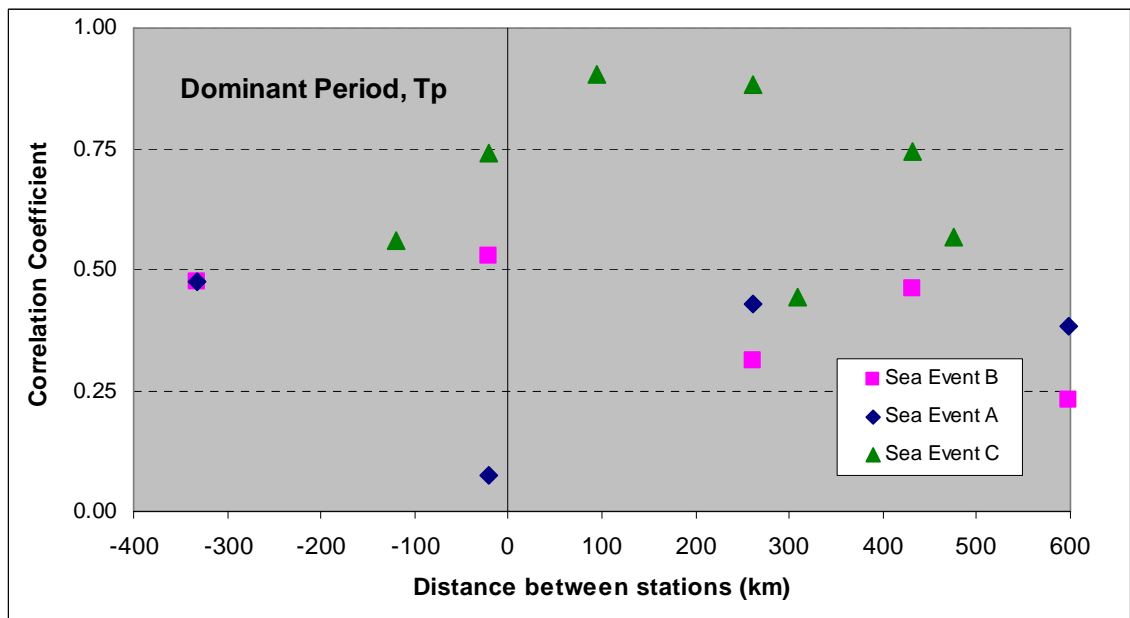


**Figure 4-24.**  
Correlation between measured dominant period at pairs of buoys as a function of the distance between buoys for three “sea events” in May through September 2007.

The coast-wise correlation of sea state parameters for local wind driven seas is highly variable, reflecting the north-south variability in high-wind events as they develop near shore or move into the coastal area. The correlation is substantially better for swell events, reflecting the stronger coherence of these long-period wave trains as they leave the highly confused (multi-directional) seas of storm areas far offshore and travel at their group velocity towards the coast, with the different harmonic components of the storm spectra sorting themselves out as longer-period components travel faster than shorter-period components, according to the dispersion relationship of linear wave theory, producing relatively coherent swell by the time they reach the coast.

Among the three sea events studied, the 75% threshold correlation coefficient value appears to be reliably exceeded only out to a distance of 100 km. Although Event C appears to correlate well out to a distance of nearly 500 km, reflecting a large wind system on the coast, the other two sea events appear to have been much more localized, and are probably more representative of how well wind sea events are correlated up and down the coast.

As already noted, swell events are correlated over a much longer distance. In all three cases, the 75% threshold correlation coefficient appears to be exceeded out to a distance of nearly 300 km.



# 5

## CONCLUSIONS

This study has met its specific objectives, as follows:

- (1) The forecast skill of NOAA’s operational WAVEWATCH III model has been evaluated in comparison with buoy-measured wave data in deep water off Washington and Oregon and shown to have an adjusted forecast accuracy up to 48-hours ahead that is very nearly as good as (for Hs) or better than (for Te) the sea state resolution with which emerging standards require wave energy device developers to specify their power output.
- (2) Measurement-to-measurement correlations between locations where WAVEWATCH III operational forecasts are available and locations where such forecasts are not available is greater than 75% up to a distance of 300 km for all swell events and some sea events, with poorer correlation for highly-localized sea events (small storms or frontal systems). This suggests that a neural network engine can be programmed to extend the “reach” of routine operational WAVEWATCH forecasts into coastal power plant locations where such forecasts are not routinely available.
- (3) The potential benefit of incorporating retrospective (“looking back at the data”) algorithms into a “self-training” neural network engine to evolve and improve wave forecasting skill is likely to be realized only in instances where correlation coefficients between forecasts and measurements or between two sets of measurements exceed 75%. In the case of routine operational WAVEWATCH III forecasts at near-shore stations, this degree of correlation exists between original forecasts and measurements out to five days ahead, suggesting that application of neural network technology would yield substantial gains in forecasting skill relative to the 48-hour skill shown for our simple adjusted forecast.
- (4) Based on the goodness of linear regression fits shown for the various data sets we evaluated (as detailed above), we conclude that “moving window” regressions are likely to yield even better fits than one fit over the entire five-month period of analysis, which is the naïve method we used to adjust our forecasts. Therefore, programming of the neural network engine for both improving operational deep-water forecast skill and extending that skill to coastal wave power plant locations should be a relatively straightforward determination of the appropriate look-back time interval for performing the regressions and the appropriate forecast adjustment interval for applying those regression relationships.



# 6

## RECOMMENDATIONS FOR FUTURE WORK

In order to progress through Stage Gate #2 and justify funding of future phases, this report answers two questions, as first presented in the Introduction. Each is asked again, and answered affirmatively, in Sections 6.1 and 6.2 below. Having cleared this stage gate, Section 6.3 makes specific recommendations for the next phase of work to be accomplished in making real-time wave forecasting a reality for grid-connected wave power management in the BPA system.

### First Stage Gate #2 Question and Answer

Is the accuracy of existing, operational WAVEWATCH III forecasts sufficiently good that any further development of a forecasting workstation for wave energy utility integration purposes should be based on this NOAA operational product?

The answer to this first question is yes. Based on emerging wave energy device performance characterization protocols, the mean absolute errors of WAVEWATCH III's adjusted forecasts for 48 hours ahead were shown to be very nearly within (in the case of  $H_s$ ) or clearly within (in the case of  $T_e$ ) one sea state bin width in the so-called "power matrix" that device developers use to characterize power output as a function of significant wave height and energy. An important corollary finding is the very high correlation (>75%) of WAVEWATCH III operational forecasts with measurements at routine output locations, suggesting that a neural network engine would be successful in adjusting future forecasts based on learning from the regression relationship between past forecasts and past measurements, with the prospect of meeting sea state parameter accuracy requirements for forecasts out to five days ahead.

### Second Stage Gate #2 Question and Answer

Is the coast-wise correlation between locations where WAVEWATCH III forecasts are available and locations where wave power plants would be sited and such forecasts are not available and neural net technology may be used to extend the "reach" of WAVEWATCH forecasts into these coastal locations?

The answer to this second question is yes. Our analysis showed a strong measurement correlation between near shore buoys (at operational WAVEWATCH III output locations) and coastal buoys (at typical wave power plant locations), exceeding 75% in all swell events and some sea events out to a distance of nearly 300 km. We judge these to be sufficiently good to warrant research into the application of neural net technology to extend the reach of WAVEWATCH III to any coastal location. Still unknown, however, is the degree to which neural net technology can achieve the required accuracy, particularly for localized wind-driven sea events.

### Recommendations for Next Phase

Our overall conclusion is that WAVEWATCH III forecasting skill, combined with the strong correlation between near-shore buoy locations where operational forecasts are available and the coastal locations of typical wave power plants, offer a wave energy forecasting capability that wave power plant owners can use for making days-ahead wave power commitments thus enhancing the value of wave power to the electricity grid.

Note that this applies only to the relatively calm summer months that coincided with our study period. We recommend archiving and analyzing the forecast skill of WAVEWATCH III in the winter months so that a full year of data is available for analysis. Virginia Tech will continue to archive real time WAVEWATCH III data into the summer of 2008 and possibly beyond. The analysis of these winter data will be recommended as part of a future proposal.

There are efforts underway to improve wave forecasts using improved physical models, such as for the Columbia River bar (Reference 9) and the entrance to Humboldt Bay (Reference 10). Such physical models are highly site-specific and require considerable “one-off” research and development effort based on the need to prepare a digitized bathymetric grid and having suitable measured directional wave data to drive the numerical simulation of refraction and shoaling and bottom friction on the directional spectrum. It is quite possible that using a neural network algorithm to extend the reach of Wavewatch III may be simpler and more universally applied.

Our second specific recommendation that would be part of any future proposal is to perform a trial-and-error (through automated simulation techniques) “march” through the full year of forecast data, trying different combinations of data look-back interval and forecast adjustment interval to determine the optimal combination that yields the highest accuracy.

# 7

## REFERENCES

- (1) Alberta Electric System Operator “Market and Operational Framework for Wind Integration in Alberta.” March, 2007.
- (2) Kariniotakis, G., P. Pinson, N. Siebert, G. Giebel, and R. Barthelmie, “The State of the Art in Short-term Prediction of Wind Power – From an Offshore Perspective.” Proceedings of SeaTechWeek, Brest, France. October 2004.
- (3) United Kingdom Department of Trade and Industry, “Preliminary Wave Energy Device Performance Protocol, Version 1.3.” Prepared by Heriot-Watt University and The University of Edinburgh. March, 2007.
- (4) European Marine Energy Centre, “Performance Assessment for Wave Energy Conversion Systems in Open Sea Test Facilities.” 2004.
- (5) H.T. Wang and C.B. Freise, “Error Analysis of the Directional Wave Spectra Obtained by the NDBC 3-m Pitch-Roll Discus Buoy.” IEEE Journal of Oceanic Engineering, Vol. 22, Issue 4, pp. 639 – 648. October 1997.
- (6) W. O'Reilly, T. Herbers, R. Seymour, and R. Guza, “A Comparison of Directional Buoy and Fixed Platform Measurements of Pacific Swell.” Journal of Atmospheric and Oceanic Technology, Vol. 13, Issue 1, pp. 231–238. February 1996.
- (7) H. Madsen. “A Protocol for Standardizing the Performance Evaluation of Short-Term Wind Power Prediction Models.” Project ANEMOS Deliverable 2.3. March 2004.
- (8) A. Debs , C. Hansen, Y. Makarov , D. Hwakins and Peter Hirsch, “Wind Power Forecasting in California based on the EPRI ANNSTLF,” paper presented at the 2004 Balkan Power Conference, Bucharest, Rumania.
- (9) Y.C. Chao and T. Bertucci, “A Columbia River Entrance Forecasting Program Development at the Ocean Products Center. National Weather Service, National Meteorological Center Office Note 361. October 1989.
- (10) T. Nicolini and G. Crawford. “A High Resolution Nearshore Wave Model for Northwestern California.” NWS Cooperative Project, UCAR Award No. S03-44676, Final Report. December 2005.



# A

## PRIMER ON WAVE ENERGY VARIABILITY

The key to effective utilization of ocean wave energy lies in understanding its variability over several time scales. Wave energy devices must be designed to absorb energy from a spectrum of individual wave heights and periods. These quantities vary randomly from one wave to the next, although this variability may not be apparent to a casual observer on shore. Indeed, such an observer is likely to be impressed by the regularity with which waves break, one after the other, in apparently monotonous succession.

The regular features of breaking waves are caused by interactions with the bottom as waves enter shallow water, and the illusion of regularity is dispelled when waves are viewed on the open ocean, away from shore. Unlike a line of breakers, waves in deep water generally appear as a confusion of hills and hollows moving in several directions at once.

Such a confused sea state is represented mathematically as the sum of several simple harmonic waves, each having a specific height, period, and direction of travel. This random superposition of regular wave components is a fundamental concept in ocean engineering and has proven to be an accurate basis for predicting the effects of natural waves on ships and offshore structures.

In order to understand random waves, then, it is first necessary to understand the properties of simple harmonic or regular waves, and these are described in the first section of this primer. The superposition of such waves, all moving in the same direction, creates a random wave train whose crests are infinite in extent. Such long-crested waves are not a natural phenomenon, but represent an intermediate step towards synthesizing a short-crested sea state.

Long-crested random waves are described in the second section of this primer, which introduces the concept of the wave spectrum. Angular spreading of the wave spectrum, with harmonic components traveling in different directions, creates short-crested waves, whose properties are described in the third section.

The first three sections of this primer deal with energy variability from wave to wave, over a time scale of seconds. Over a longer time scale, on the order of minutes, it is frequently observed that wave energy arrives off the coast in successive groups of high and low waves, a phenomenon well known to any surfer. Such wave grouping is described in the fourth section.

Finally, over a time scale of hours to days, the natural wave power density at a given location changes in response to local wind conditions and the arrival of swell from offshore storms. The factors that influence such changes in sea state are described in the last section of this primer and are an important consideration for wave power plant operators, who must continually “tune” the plant to changing sea states, and to utility dispatchers concerned about variability in plant output.

## **Regular Waves**

A simple harmonic water wave is described primarily by three parameters (Figure A-1): its height ( $H$ ), which is the vertical distance from crest to trough; its wavelength ( $L$ ), which is the horizontal distance from one crest to the next; and its period ( $T$ ), which is the length of time it takes for two successive crests (or any other phase of the wave) to pass a fixed point. Once a regular wave has been generated, its period remains constant, but its height and length are affected by the water depth in which it travels.

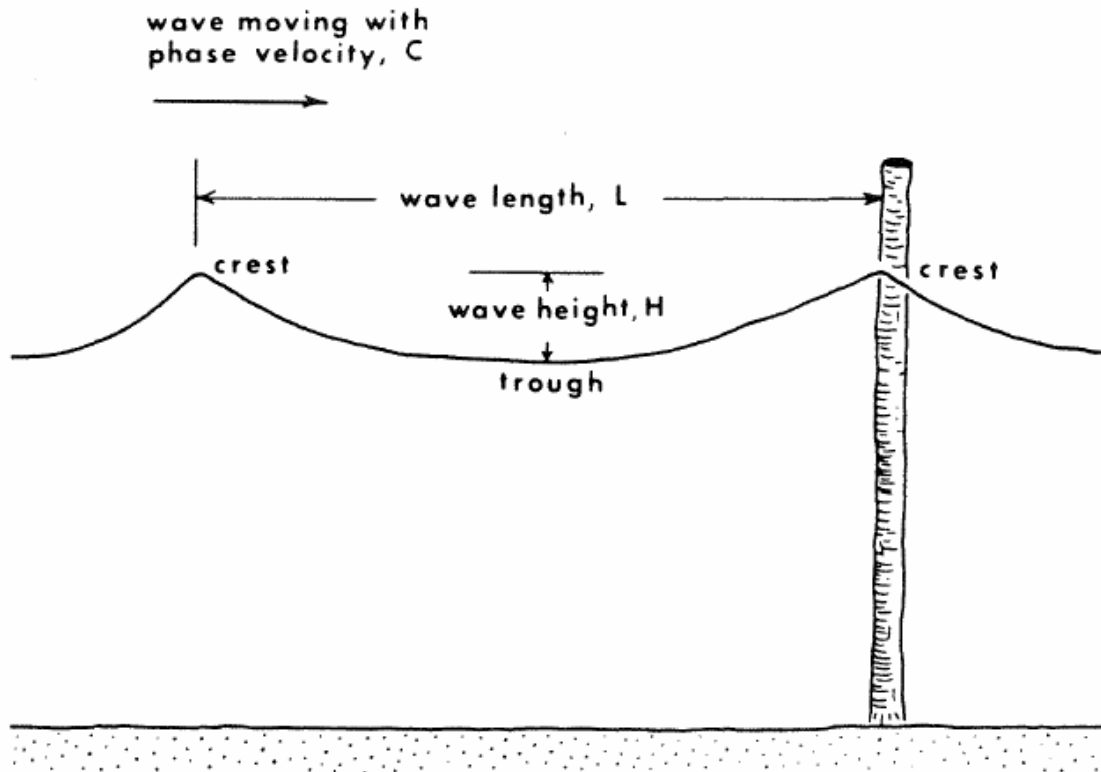


**Figure A-1.**  
**Definition sketch for regular wave parameters.**

If one observes the motion of a floating object during the passage of regular waves in deep water, it will be seen that the object rises and falls, but makes no net progress in the direction of wave travel. This is because the changing sea surface slope of the passing wave induces hydrodynamic pressure gradients that accelerate the object and sub-surface water particles in circular orbits. Waves therefore transfer energy without transferring mass; to a first approximation, the water itself does not travel with the wave.

At the sea surface, the diameter of water particle orbits is equal to wave height. Orbital motion decays exponentially with depth, and half a wavelength down, its amplitude is only 4% of its surface value, and the wave is not affected by the bottom in water deeper than half a wavelength. In deep water, wavelength is directly proportional to wave period squared. Thus, as shown in Table A-1, a 10-second wave is four times longer than a 5-second wave, and it will begin to feel



the bottom in water that is four times as deep. Since the rate at which a wave travels (its phase velocity) is equal to wavelength divided by period, it travels twice as fast.

**Table A-1.**  
**Regular Wave Comparison for Three Different Periods**

| Wave period:  | <u>5 sec</u> | <u>10 sec</u> | <u>15 sec</u> |
|---|--------------|---------------|---------------|
| Deep water wavelength:                                    | 39 m         | 156 m         | 351 m         |
| Deep water phase speed:                                   | 7.8 m/sec    | 15.6 m/sec    | 23.4 m/sec    |
| Depth at which wave begins<br>to be affected by seafloor: | 20 m         | 80 m          | 175 m         |

continually appear at the rear of the group, grow to full height as they travel through the group, and die away at the group's leading edge.

This phenomenon is a consequence of the way in which energy is partitioned in a wave and how it is transmitted across the water. Half of the wave's energy is always stored in potential form, associated with the vertical rise and fall of the water surface from its still-water condition. The other half is expressed as kinetic energy, associated with the orbital motion of water beneath the wave. Because the orbits are circular, kinetic energy does not travel with the wave, and only the wave's potential energy travels at phase velocity.

Consider a group of regular waves traveling into previously undisturbed water (Figure A-2). Only the potential energy of the leading wave travels at phase velocity, and there is a reduction in wave height as half of this is converted to kinetic energy when the sub-surface water particles, which were at rest, are set into motion. The remaining half is available to travel the next wavelength, where it again is used to supply kinetic energy to the undisturbed water. This conversion of potential to kinetic energy continues until the first wave is too small to identify.

Since the leading wave has left all of its original kinetic energy behind, the second wave to follow does not lose any of its potential energy when it occupies the leading wave's first position. At the next position, where the leading wave lost half of its potential energy, the second wave loses only a quarter in order to maintain an equal balance of potential and kinetic energy throughout the wave group. Successive waves lose potential energy at an even lower rate as they progress through the group, building on the kinetic energy left behind by previous waves. They begin to lose height quickly, however, when they reach the group's leading edge and move into undisturbed water.

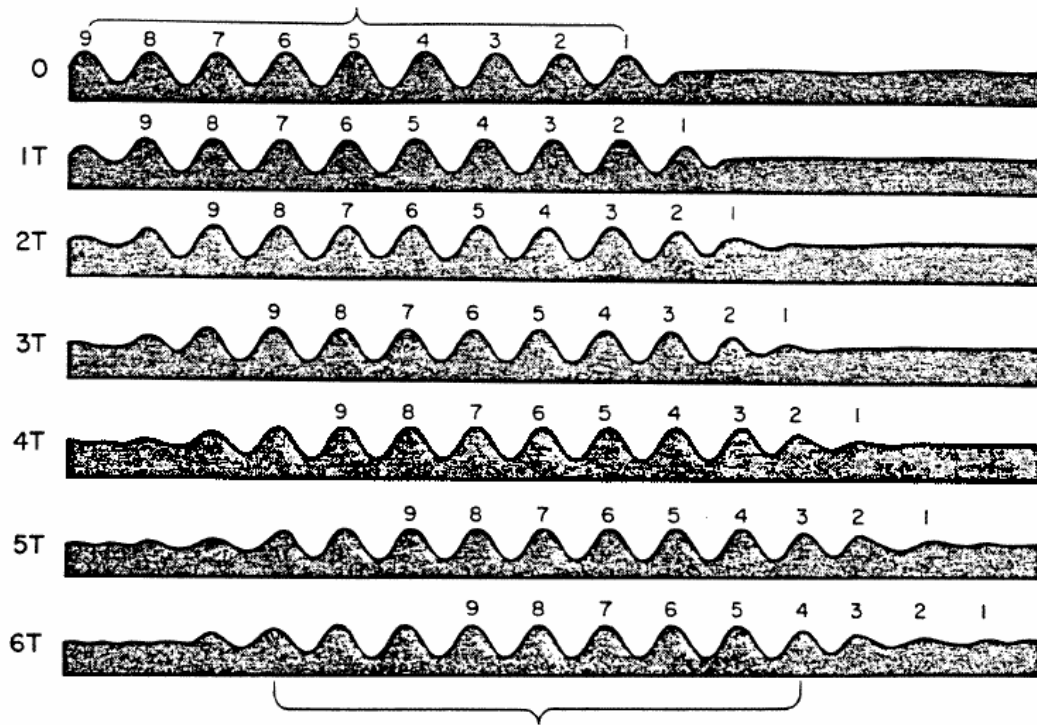


**Figure A- 2.**

**The advance of regular waves into still water.**

Each successive position corresponds to a time increment of one wave period ( $T$ ). Note that at time  $6T$ , each individual wave has traveled six wavelengths, while the wave group has advanced only three wavelengths. Also note that at time  $6T$ , the leading wave retains only  $1/64$  of its original energy and has virtually disappeared.

At the rear of the group, all of the last wave's potential energy travels ahead at phase velocity. Half of the remaining kinetic energy is converted to potential energy as a crest and trough are formed by the relict orbital flow pattern. This new wave then travels ahead at phase velocity, gaining potential energy as it travels towards the group's center and losing it as it travels towards the group's leading edge. This process redistributes kinetic energy from the rear of the group to its front. Thus, the combined potential and kinetic energy of the waves travels at the velocity of the wave group, which in deep water is equal to half the phase velocity.

**Long-Crested Irregular Waves**

If several sinusoidal waves traveling in the same direction are superimposed on one another, an irregular wave profile is generated (Figure A-3). This same irregular wave profile can be separated back into its harmonic components by Fourier analysis. Each component contributes a certain amount to the total variance of the sea surface. This contribution is proportional to the square of the component's wave height, which in turn is proportional to its energy content.

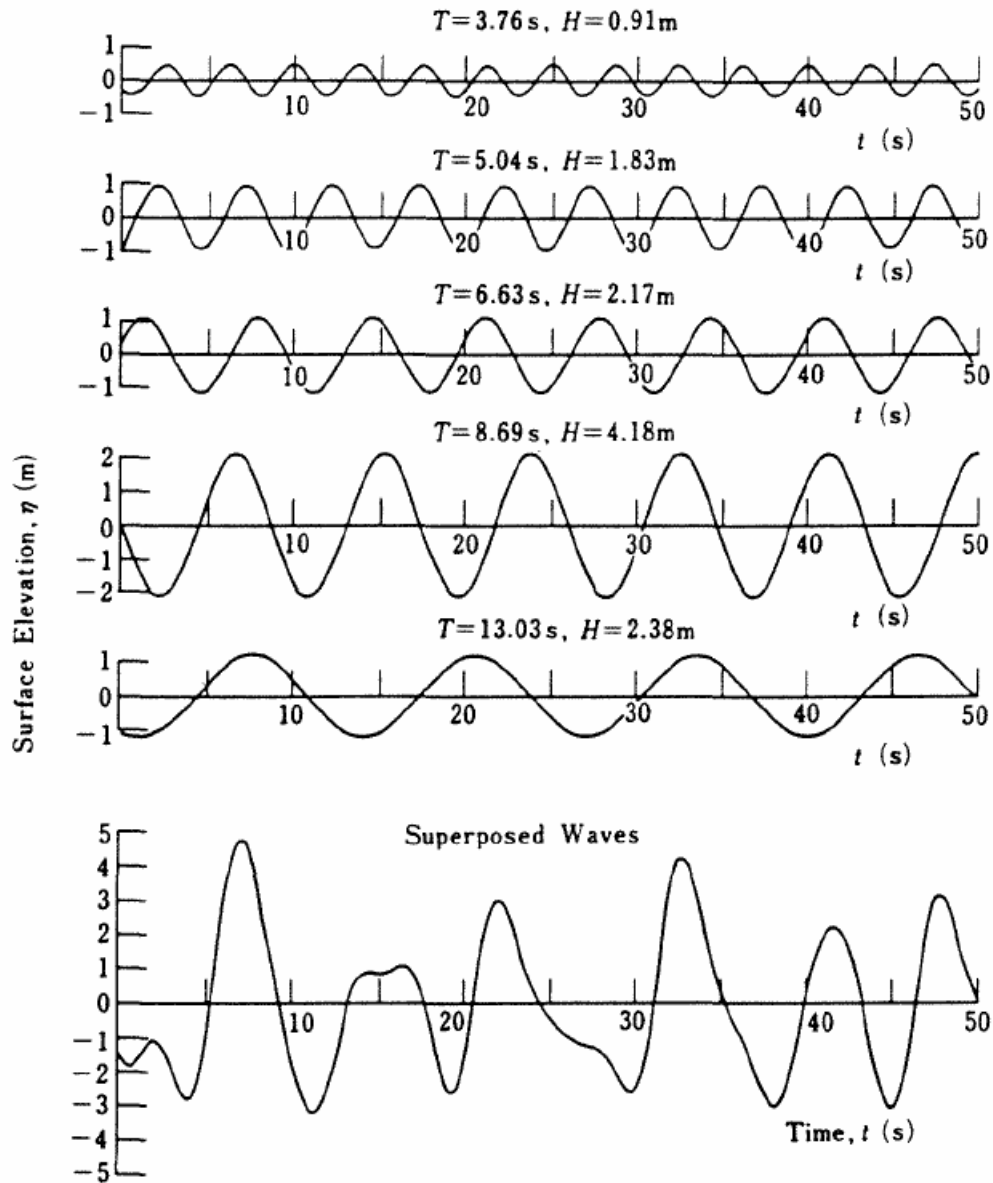


**Figure A-3.**  
**Superposition of five regular waves.**

When the sea surface variance contributed by a given harmonic component is divided by the frequency of that component and plotted as a function of wave frequency, the resulting curve is referred to as the sea surface variance density spectrum, or more simply, the “wave spectrum.” Note that the area under the spectrum curve is equal to the total sea surface variance, and the square root of this area equals its standard deviation.

When multiplied by the density of seawater and acceleration due to gravity, the area under the wave spectrum curve also represents the total energy per unit area of sea surface. Wave energy conversion devices are oriented so as to intercept this energy as it travels at the group velocity of its harmonic components. The amount of wave energy to cross a vertical plane per unit time is referred to as wave energy flux or incident wave power density, and is generally expressed in units of kilowatts per meter of wave crest. This is equivalent to megawatts per kilometer of coastline, as might be used when evaluating the wave energy resource base at a regional scale.

The concept of significant wave height ( $H_s$ ) is one of considerable importance. It is formally defined as the average height of the highest one-third waves in a given sea state and has been found to generally correspond to the wave height estimated by visual inspection of the sea surface. This is because an observer on a ship or pier tends to overlook the small waves and notice only the larger ones when visually estimating wave heights.

Just as a given sea state is characterized by its significant wave height, it is also characterized by some sort of statistically meaningful wave period. This may be the average wave period determined from zero-crossing analysis. More relevant to wave energy conversion is the dominant wave period ( $T_p$ ). This is the inverse of the frequency at which the spectrum has its highest peak. Its physical meaning is that it represents the harmonic component having the greatest amount of wave energy in a random seaway.

It should be noted that significant wave height can be rather closely estimated as four times the square root of the area under the wave spectrum. Since the total energy content of the sea surface is proportional to the area under the spectrum, then it is proportional to significant wave height squared. Furthermore, the group velocity of the most energetic harmonic component is directly proportional to dominant wave period. Therefore, to a first approximation, the energy flux in random waves is proportional to the product of  $(H_s)^2$  and  $T_p$ .

### **Short-Crested Irregular Waves**

Up to this point, the discussion of random waves has assumed that all harmonic components are traveling in the same direction, such that the waves have infinitely long crests traceable from horizon to horizon. Due to the veering and gusty nature of the wind, however, components are generated that actually travel in several directions at once. Real wave crests are thus finite in width and continually appear and disappear as the various directional components move into and out of phase with one another.

The variance density of such a short-crested random seaway is a function of both the frequency and direction of its harmonic components. This function is known as the directional wave spectrum, which is three-dimensional, as shown in Figure A-4.

Considering the short-crested nature of real ocean waves, the definition of wave power developed earlier, for long-crested waves, now requires modification. It is more correctly defined as the amount of wave energy to cross a circle one meter in diameter in one second. Although still expressed in units of kilowatts per meter, this definition does not imply that the energy is

traveling in only one direction (as it does with long-crested waves), and a vertical plane bisecting the circle may experience wave energy flux from both sides at once.

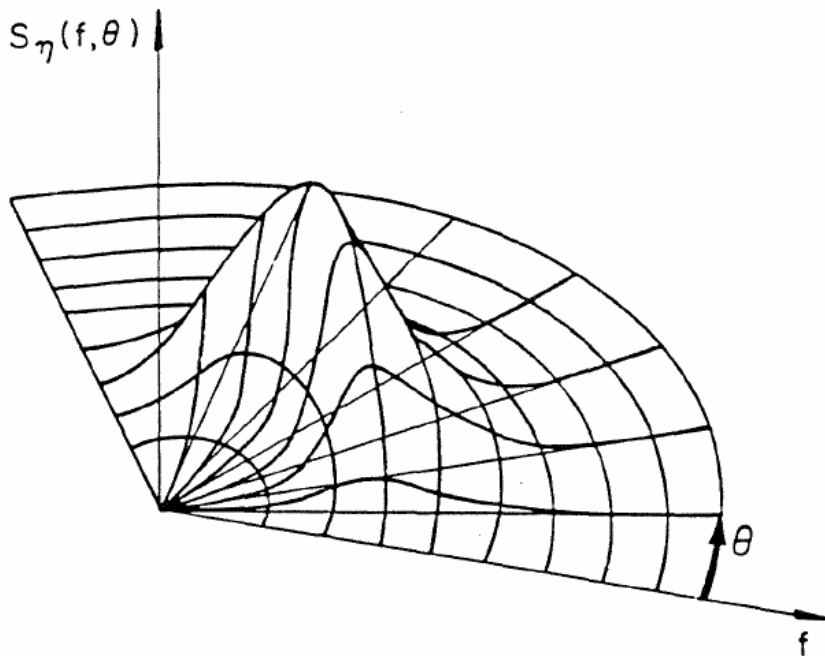


**Figure A-4.**  
**Directional wave spectrum.**

This is particularly true where winds have recently experienced a major shift in direction such that newly developing waves are crossing the older waves at a wide angle. This may also occur when swell from a distant storm is arriving from a direction that is different from that of the local wind. In such cases, two or more distinct wave trains may exist, each with its own spreading function, and the total directional spectrum may wrap more than  $180^\circ$  around the circle. An example of this is given for a NOAA data buoy location in Hawaii (Figure A-5), where two different long-period swell trains from the North Pacific and Southern Ocean are traveling in opposite directions, superimposed on a local sea built up by trade winds from the east.

### **Wave Grouping**

Although individual wave height and period vary randomly from one wave to the next, waves often occur in successive groups of alternately high and low waves. An example of such wave grouping is given in Figure A-6, which shows a 30-minute record from the Pacific coast of Costa Rica. Although the record as a whole can be described by a single wave spectrum and has an average wave power, one can see minutes-long bursts of high wave energy separated by somewhat shorter periods of relative calm

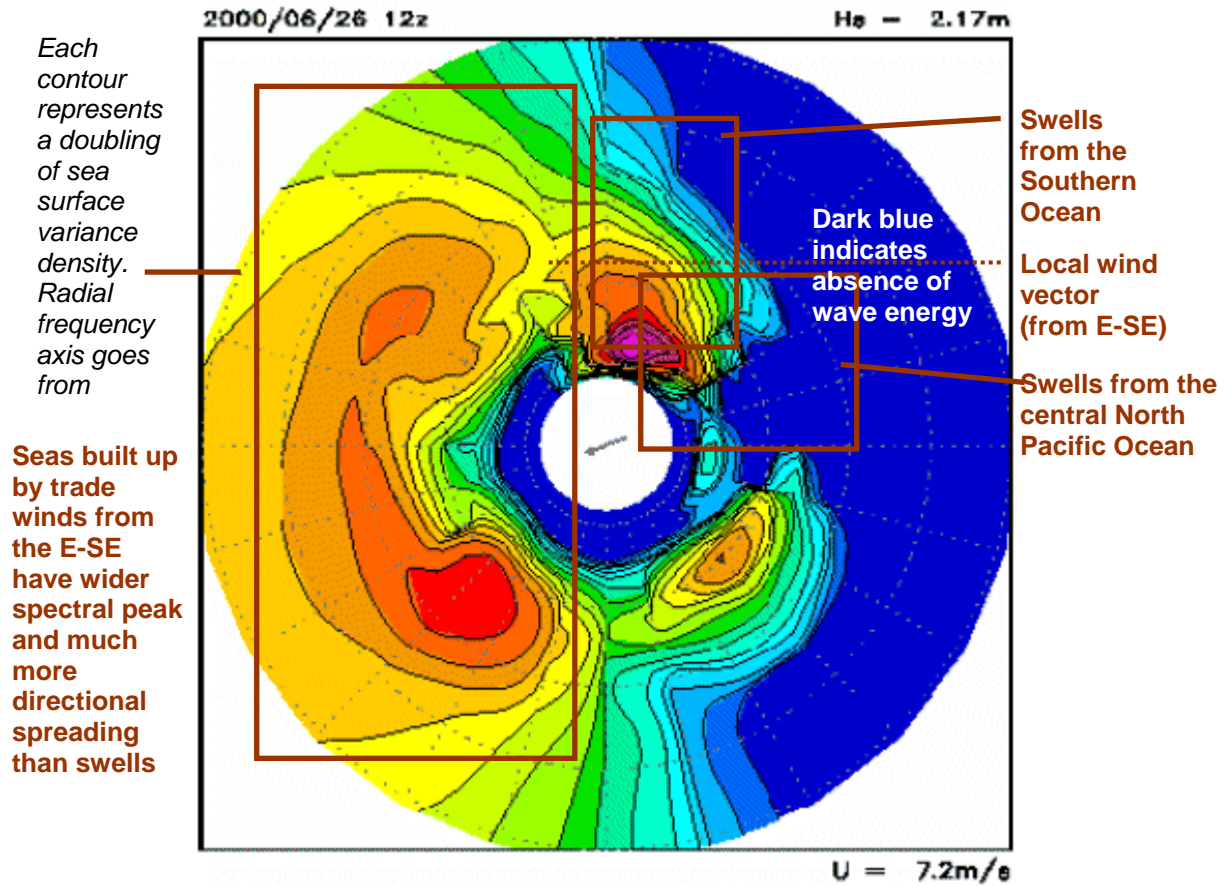


**Figure 5.**  
Example directional spectrum from deep water near Hawaii.

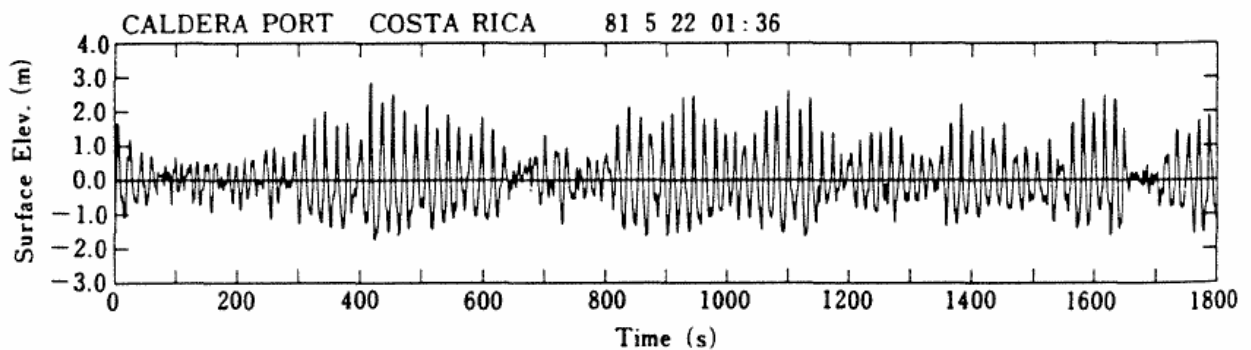


**Figure 6.**  
Example of wave grouping in swell from the Southern Ocean.

The output of wave energy conversion devices will tend to follow the envelope or profile of such wave. Means of smoothing this output, such as flywheels or hydraulic accumulators, may be a necessary first step in power conditioning for the utility grid.

It should be noted that little can be learned about wave grouping from examination of a wave spectrum, which is strictly in the frequency domain. Grouping analysis requires preservation of the time history record.

As part of the design process for a wave energy conversion device, a physical or numerical model of the device should be exercised in a series of random wave tests that covers a range of wave grouping. This will ensure that all power conversion equipment has been properly sized to handle the bursts of high wave energy and intervening low-energy periods. It should also satisfy the utility that its power quality requirements will be met throughout the entire wave sequence.

### **Changes in Sea State**

In order to appreciate the factors that influence changes in wave energy flux over hours to days, it is helpful to understand the mechanisms by which waves are generated. Consider an area of the sea surface whose initial condition is one of flat calm or low ground swell from some far-distant storm. Even if low swell is present, the sea surface itself is glassy smooth, and there is no wind.

As a breeze develops, ephemeral and quickly moving patches of ruffled water, known as “cat’s paws” appear wherever a gust brushes the water surface. These are small capillary waves, and when the local gust dies away, the glassy smoothness of the sea state is restored almost immediately. If the average wind speed increases to approximately 1.1 m/sec (2 knots) ripples develop, covering the entire area. These are the first true gravity waves, and the height to which they grow depends on the speed of the wind, the duration for which it blows, and the downwind extent (or fetch) of the area over which it is blowing.

The growth of any harmonic component in a developing random sea follows the pattern illustrated in Figure A-7. Note that either fetch or duration may limit wave growth before it reaches equilibrium. If the wind stops blowing, wave growth will stop. Likewise, in a limited fetch, waves will be exposed to the wind for only a short time before leaving the area, no matter how long the wind blows. Assuming that wave generation is neither fetch- nor duration-limited, however, the growth pattern is as described below.

A component begins to grow rapidly (transition to exponential stage) when the curvature of the air flow over the wave reaches some critical value: the steeper the wave, the more curved the wind streamlines, the greater the rate of wave growth. Since shorter-period waves attain this critical steepness at a lower height than longer-period waves, these are the first to grow exponentially. Later, given sufficient wind duration and a great enough fetch length so that the longer-period waves don’t leave the area before they reach critical steepness, they too will begin to grow exponentially.

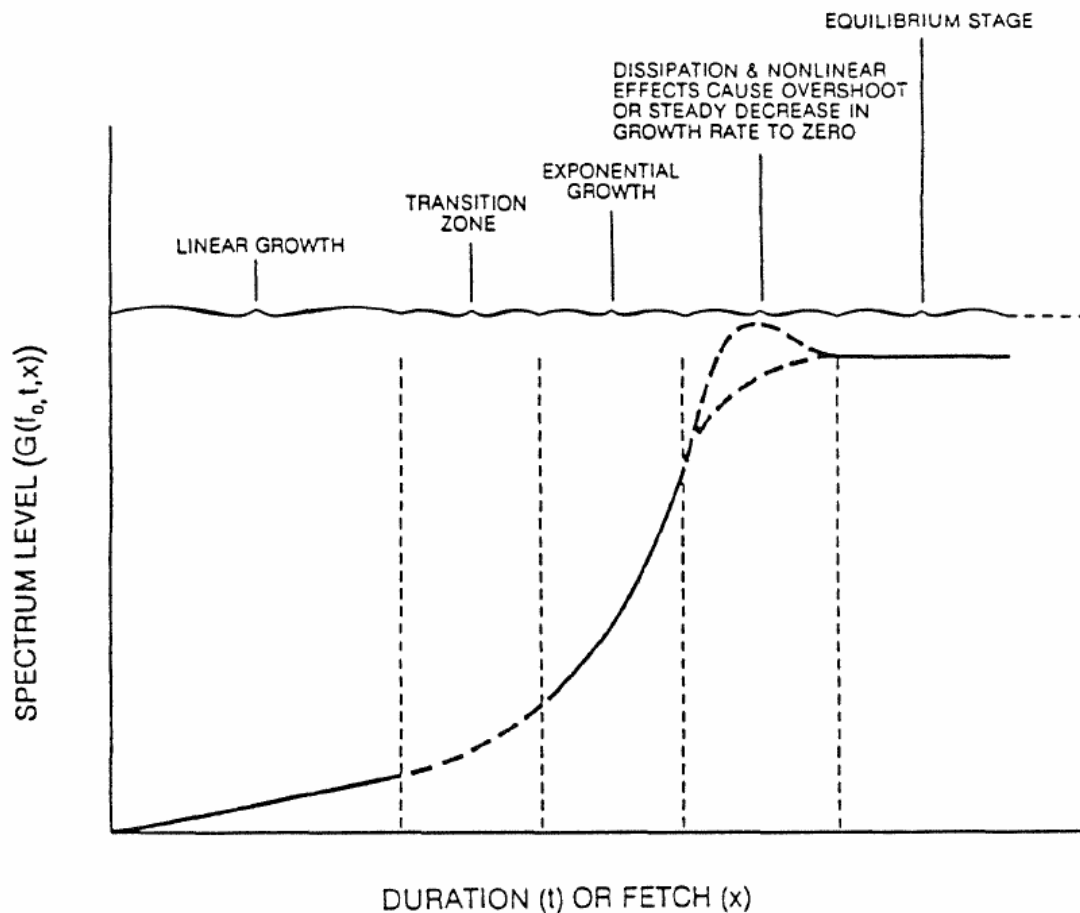


**Figure 7.**  
**Growth of an individual harmonic wave component in a developing random sea.**

Meanwhile, the shorter-period waves will have reached equilibrium height, such that any more energy supplied by the wind is dissipated or transferred to longer-period waves. Once a component has attained equilibrium, it cannot grow much higher without becoming unstable and breaking. Whitecaps may form as shorter-period waves break on the crests of longer-period waves, imparting their momentum to them and accelerating the transfer of high-frequency energy to lower frequencies.

The delayed exponential growth of lower-frequency waves and the transfer of energy from higher-frequency waves once they've attained equilibrium causes the sea state to gain energy only at frequencies below the spectral peak. Thus a wave energy conversion device situated in an actively developing sea will experience a gradual increase in dominant wave period.

Because group velocity is inversely proportional to wave frequency, there exists a low-frequency cut-off below which the energy would always be traveling faster than the wind. Thus at some point in the development of the spectrum, the waves will stop growing, even if the wind



continues to blow and the fetch is unlimited. The sea is then said to be “fully developed” for that particular wind speed. The higher the wind speed, the lower the cut-off frequency (since faster wind can keep up with faster waves), and the greater the amount of wave energy that can be contained in the fully developed sea.

Although waves are generated by the wind, high levels of wave energy can be present at a particular coastal location even in the absence of strong winds. This occurs when swell from a distant storm arrives at the coast. Swell waves tend to be more uniform in period (narrower spectrum) than those in a wind-driven sea. This is a consequence of wave dispersion, which occurs once the waves leave an area of wind generation, as described below.

Wave components of every frequency are present in a wind-driven sea. To a first approximation, the energy contained in each harmonic component travels independently, at its own group velocity. Although the different components start out together upon leaving the generation area, the longer-period waves travel faster and soon outdistance their shorter-period counterparts. The energy of the fully developed sea is thus dispersed along a corridor emanating from the generation area. The effect is similar to that of a prism, which spreads white light into several different bands of color, each one of a different constituent wavelength.

A wave gage moving at the group velocity of the peak spectral frequency would show a decrease in total energy and a narrowing of the spectrum as the shorter-period waves are left behind. A fixed gage (or wave power plant) located in the path of these waves experiences a rather abrupt increase in dominant wave period as the first, longest-period swell arrives. The dominant wave period then shifts gradually downward as the slower, shorter-period waves arrive.

Once the components of a wind-driven sea have dispersed and are well away from the generating area (500-1000 km distant), they travel thousands of kilometers with little loss of energy and can retain their identity over the span of an entire ocean basin. Even the longest waves do not begin to “feel the bottom” until they enter water depths of 300 m or less. Consequently, wave energy generated anywhere within an ocean basin ultimately arrives at some island or continental margin of that basin, virtually undiminished.



# ***B***

## **SPECTRAL ANALYSIS AND SEA STATE PARAMETER ESTIMATION**

**[Insert Heading—if needed] Heading, Level 7**

*[Copy and paste text from original file]* aliquip ex ea commodo consequat. Duis autem vel eum iriure dolor in hendrerit in vulputate velit esse molestie consequat



# C

## COMPLETE RESULTS FOR FORECAST AND MEASUREMENT CORRELATIONS

Mean absolute error (MAE) for all four sea state parameters are plotted in three figures per station, as follows:

Station 46002: Figures C-1 through C-3

Station 46005: Figures C-4 through C-6

Station 46022: Figures C-7 through C-9

Station 46029: Figures C-10 through C-12

Station 46050: Figures C-13 through C-15

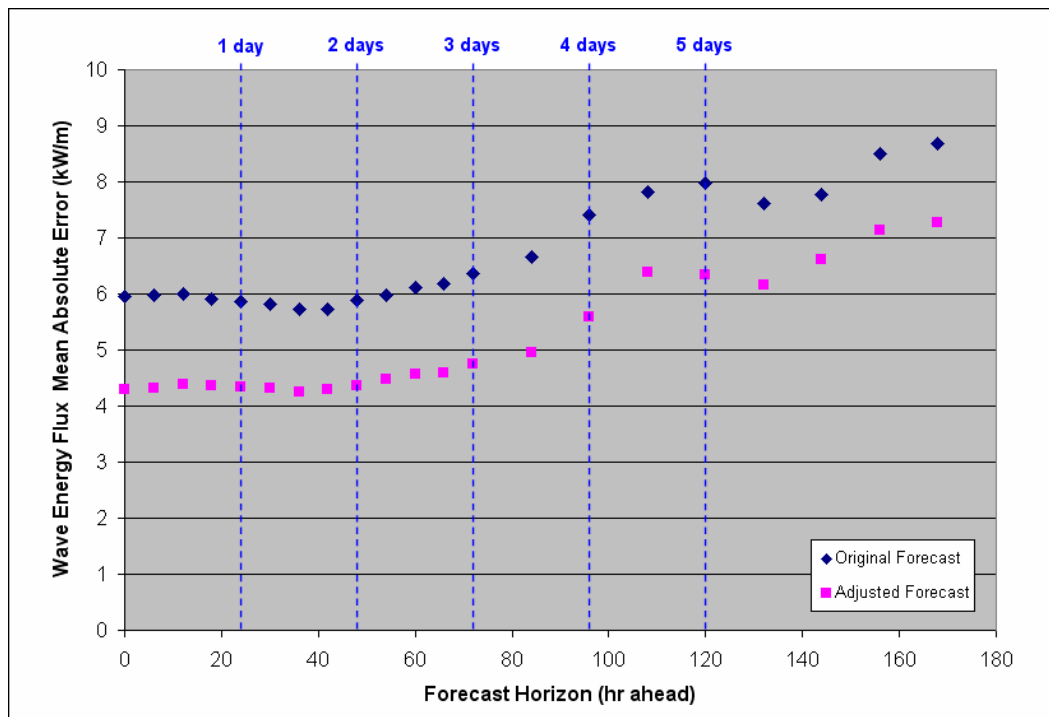


**Figure C-1.**

**Mean absolute error of WAVEWATCH III forecast for wave energy flux at NDBC Station 46002 during the period from 24 May through 30 September 2007.**

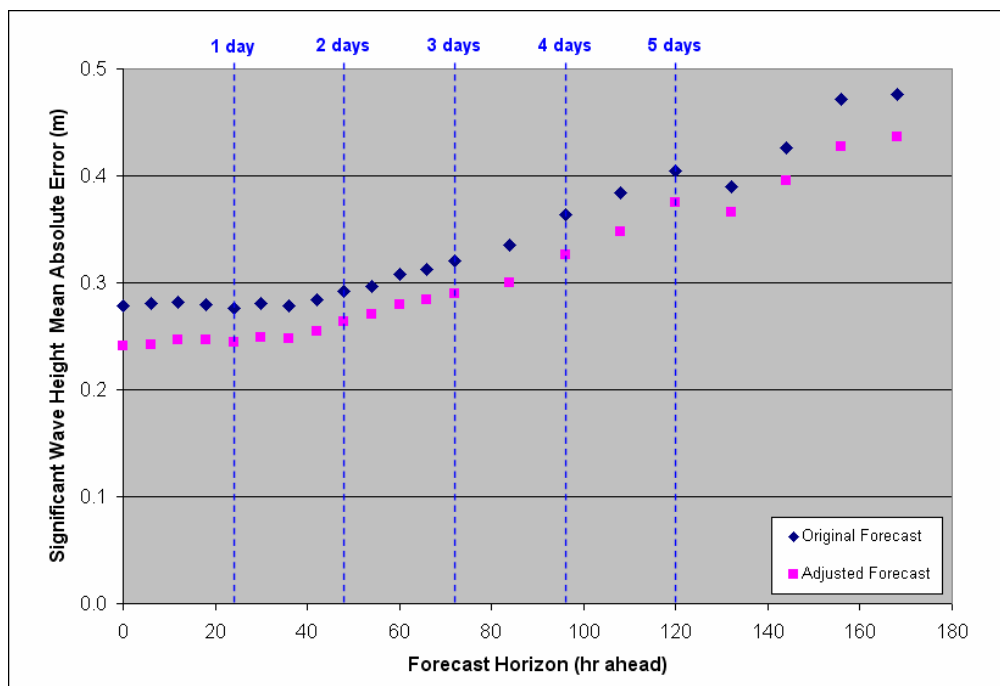


**Figure C-2.**  
Mean absolute error of WAVEWATCH III forecast for significant wave height at NDBC Station 46002 during the period from 24 May through 30 September 2007.

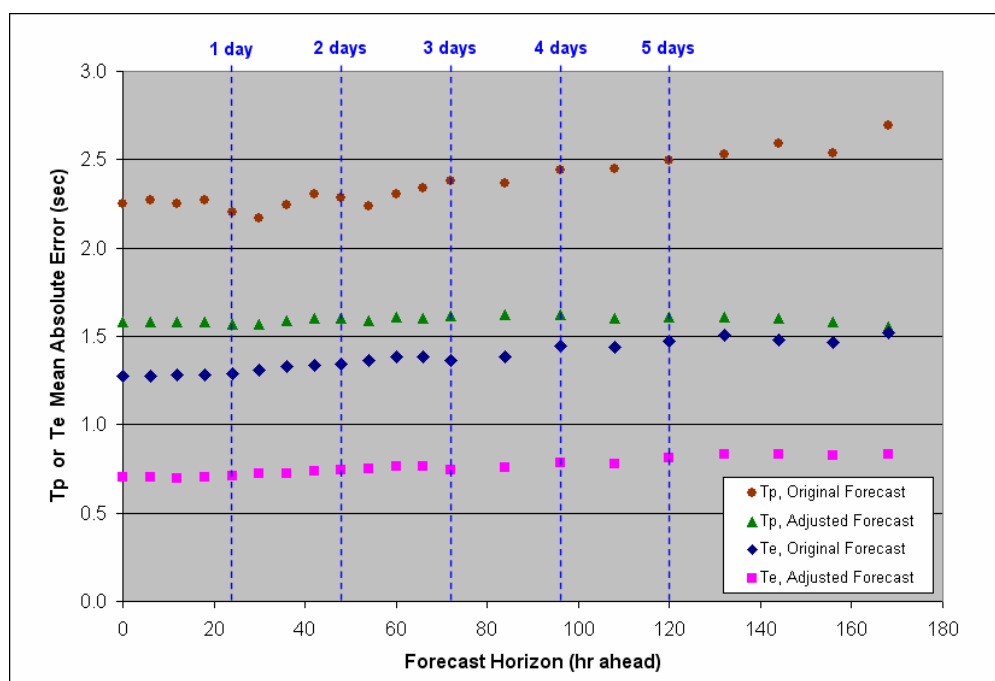


**Figure C-3.**  
Mean absolute error of WAVEWATCH III forecast for two wave period parameters at NDBC Station 46002 during the period from 24 May through 30 September 2007.

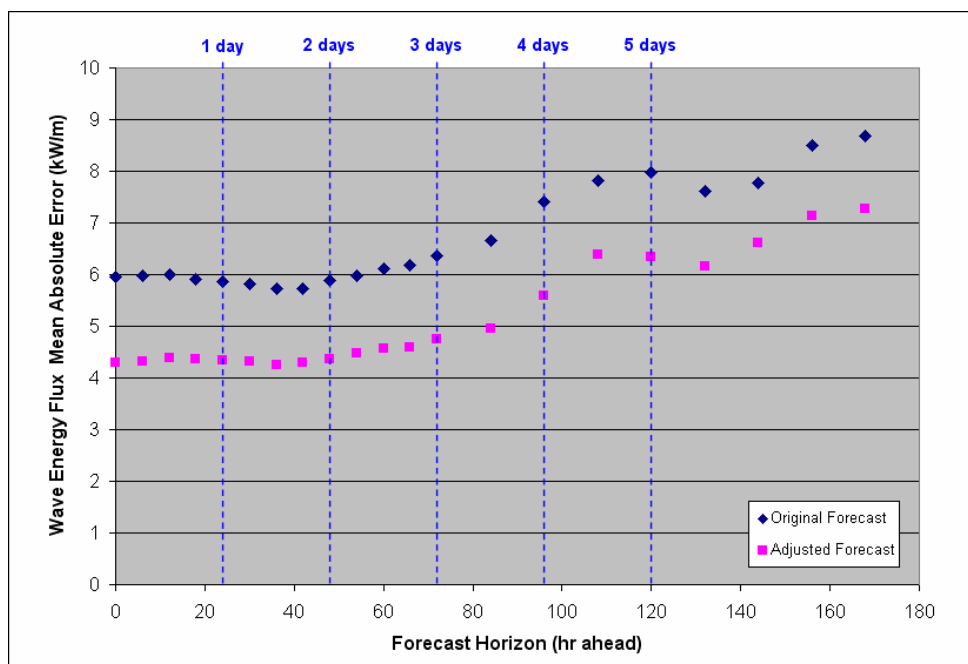


**Figure C-4.**  
**Mean absolute error of WAVEWATCH III forecast for wave energy flux at NDBC Station 46005 during the period from 24 May through 30 September 2007.**

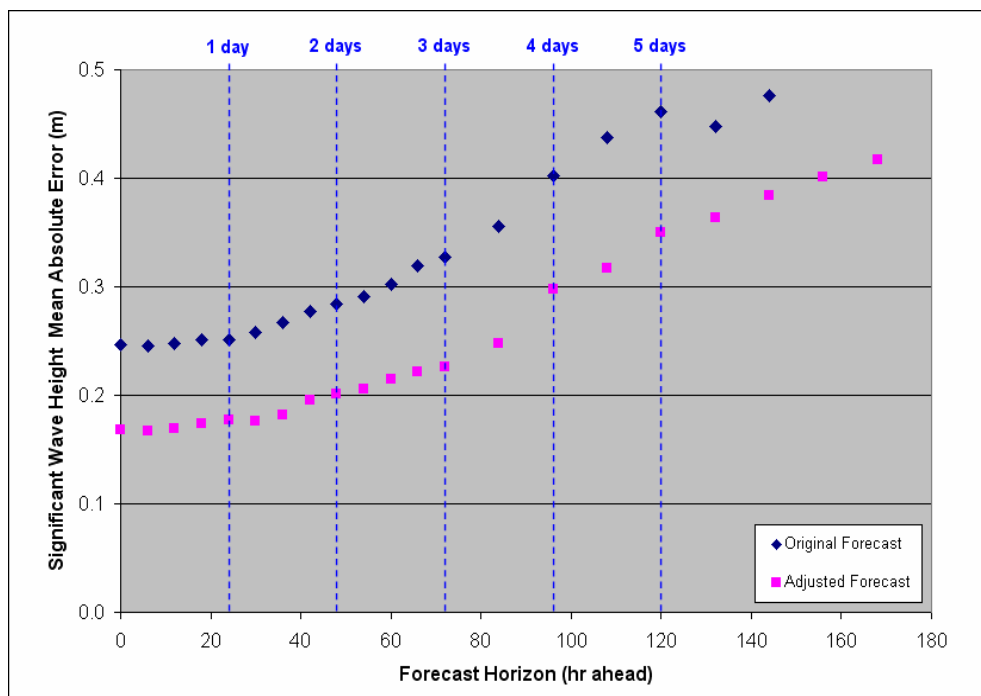


**Figure C-5.**  
**Mean absolute error of WAVEWATCH III forecast for significant wave height at NDBC Station 46005 during the period from 24 May through 30 September 2007.**

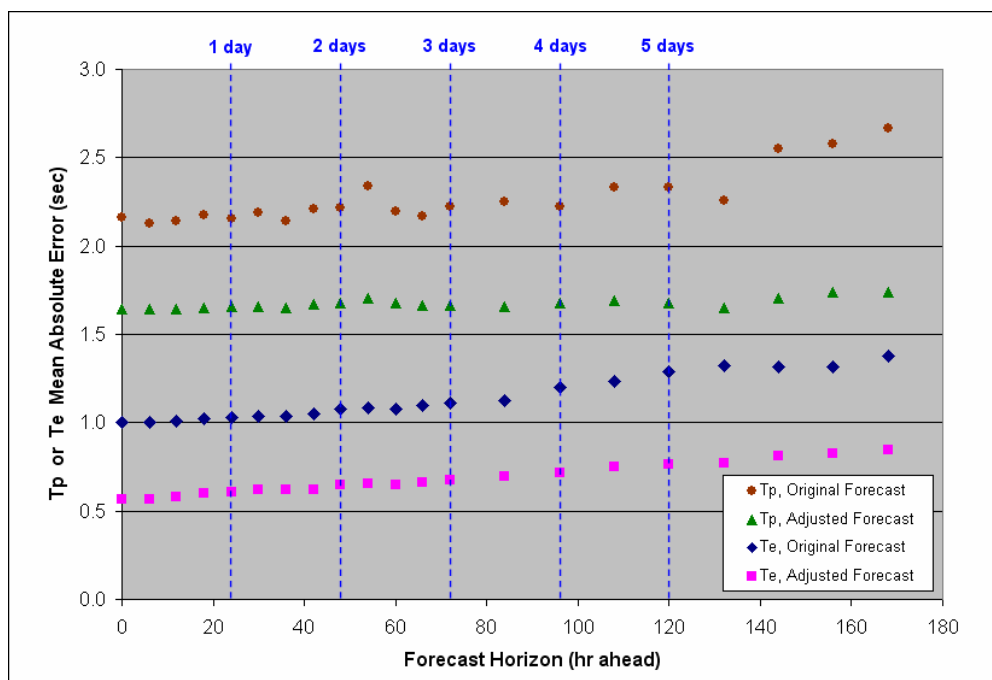


**Figure C-6.**  
Mean absolute error of WAVEWATCH III forecast for two wave period parameters at NDBC Station 46005 during the period from 24 May through 30 September 2007.

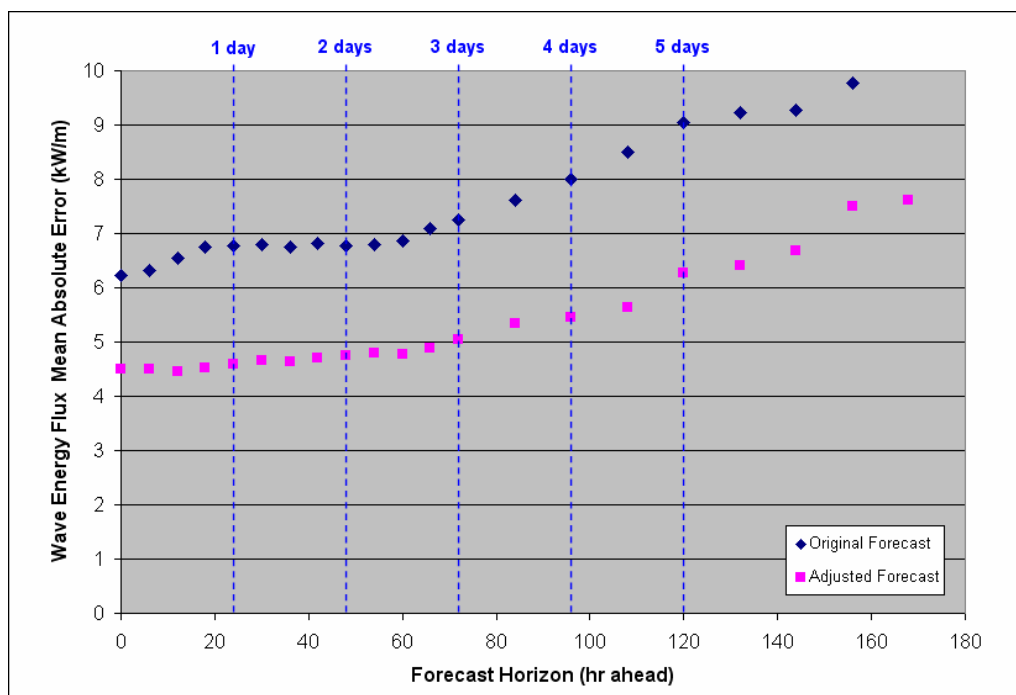


**Figure C-7.**  
Mean absolute error of WAVEWATCH III forecast for wave energy flux at NDBC Station 46022 during the period from 24 May through 30 September 2007



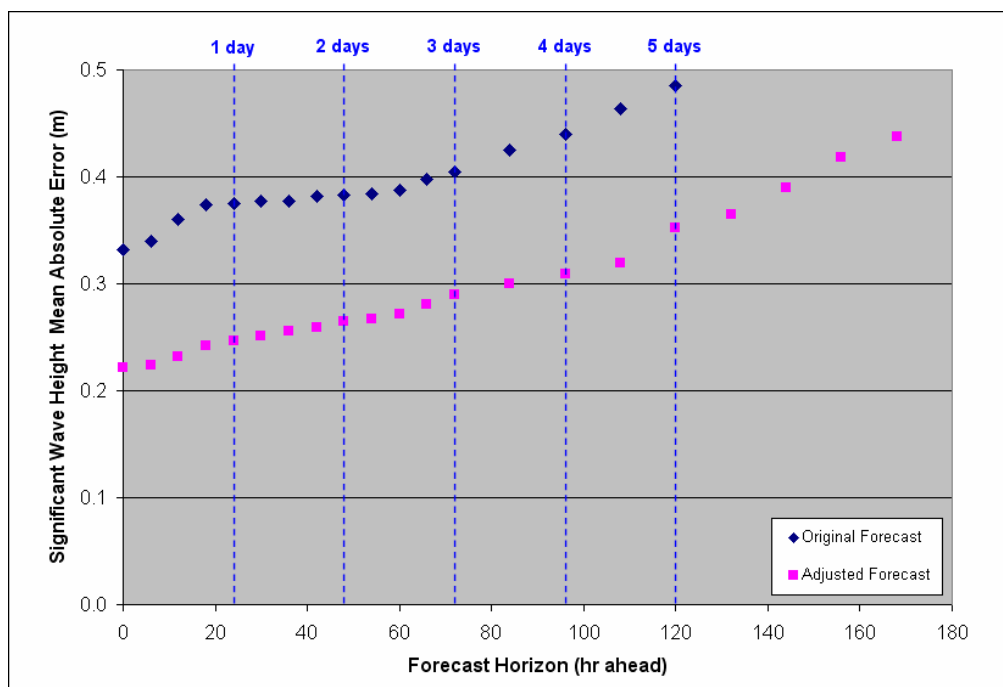


**Figure C-8.**  
Mean absolute error of WAVEWATCH III forecast for significant wave height at NDBC Station 46022 during the period from 24 May through 30 September 2007.

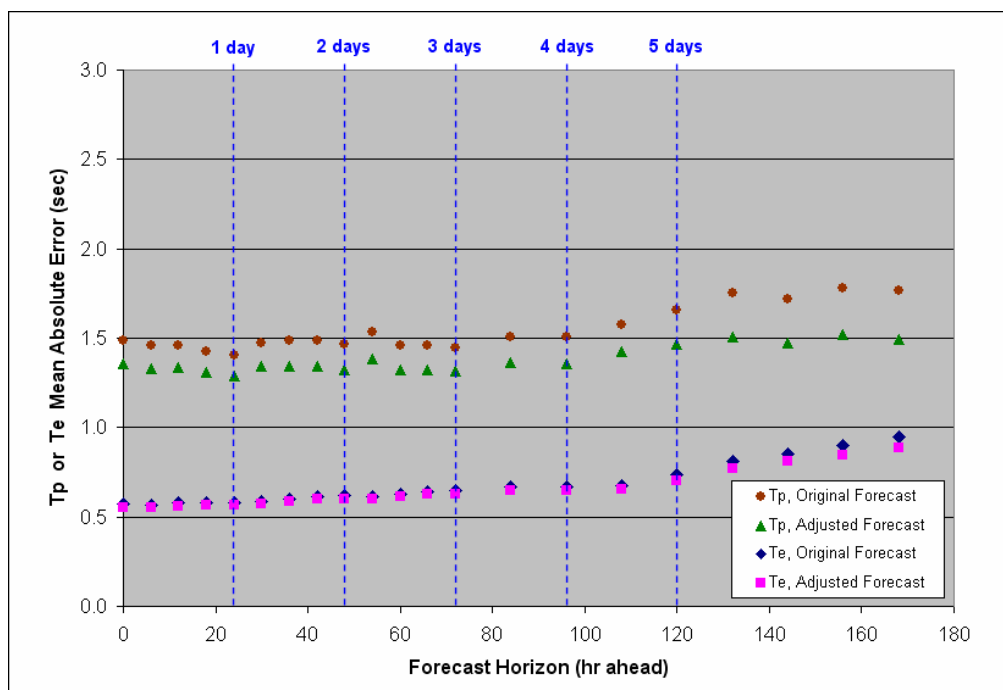


**Figure C-9.**  
Mean absolute error of WAVEWATCH III forecast for two wave period parameters at NDBC Station 46022 during the period from 24 May through 30 September 2007.

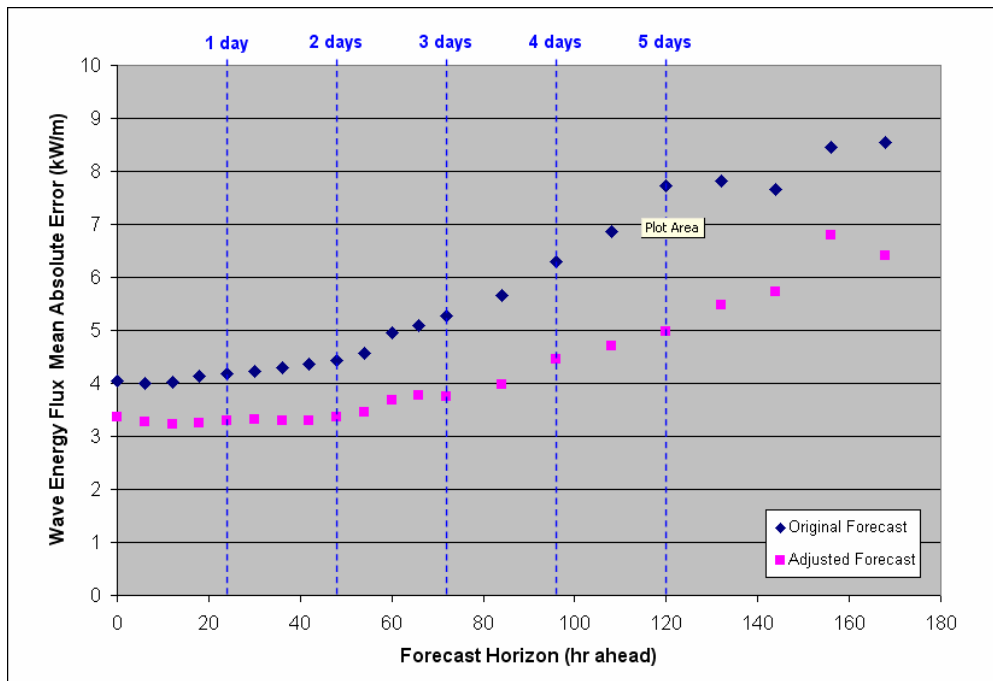


**Figure C-10.**  
Mean absolute error of WAVEWATCH III forecast for wave energy flux at NDBC Station 46029 during the period from 24 May through 30 September 2007.

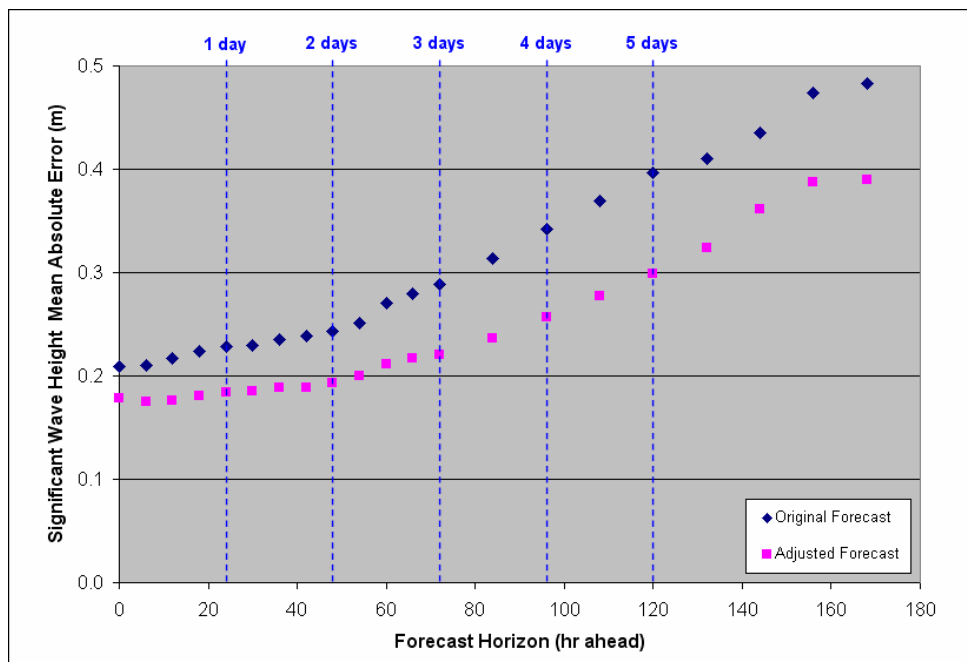


**Figure C-11.**  
Mean absolute error of WAVEWATCH III forecast for significant wave height at NDBC Station 46029 during the period from 24 May through 30 September 2007.

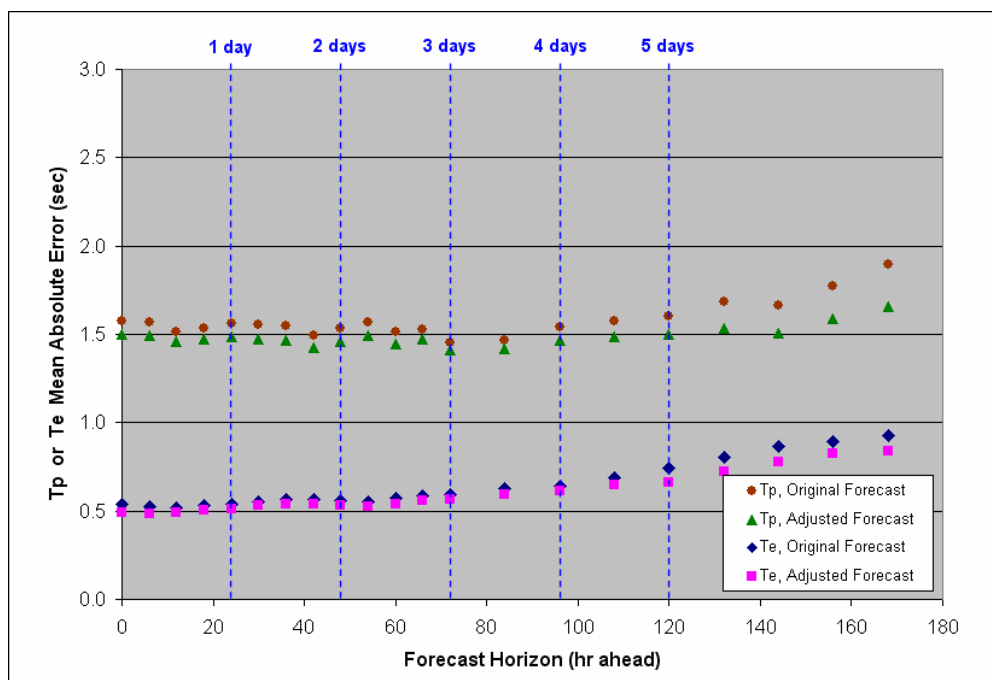


**Figure C-12.**

Mean absolute error of WAVEWATCH III forecast for two wave period parameters at NDBC Station 46029 during the period from 24 May through 30 September 2007.

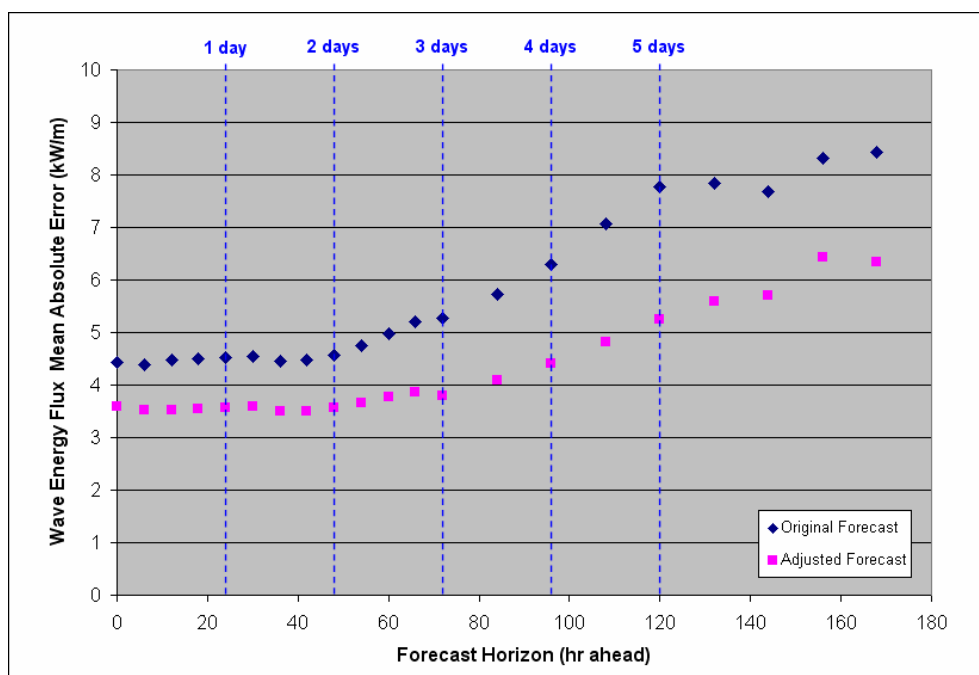


**Figure C-13.**

Mean absolute error of WAVEWATCH III forecast for wave energy flux at NDBC Station 46050 during the period from 24 May through 30 September 2007.

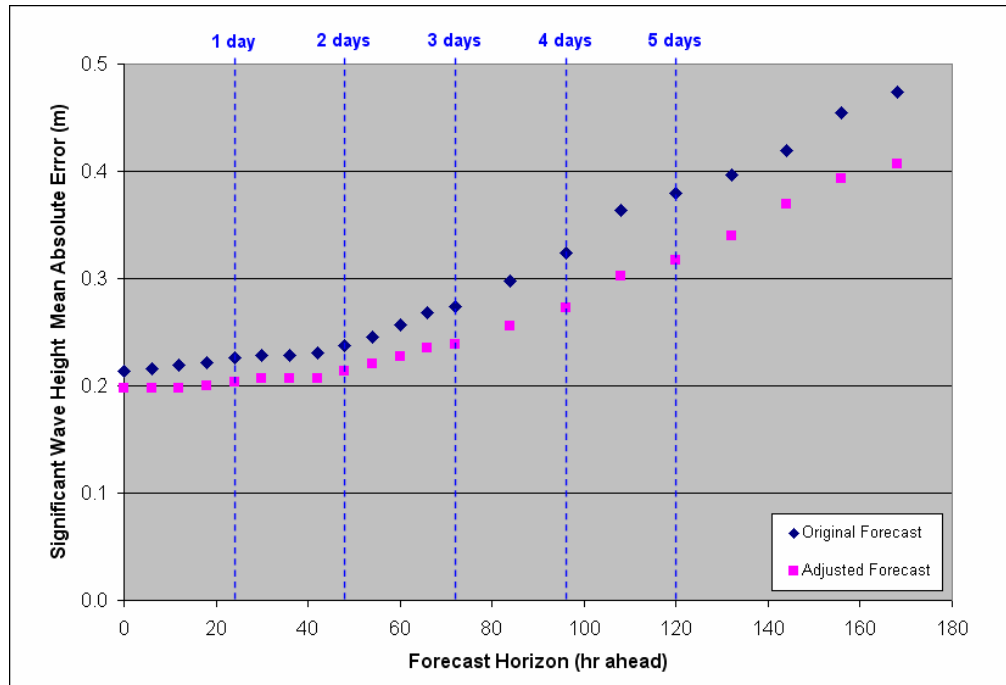


**Figure C-14.**  
Mean absolute error of WAVEWATCH III forecast for significant wave height at NDBC Station 46050 during the period from 24 May through 30 September 2007.

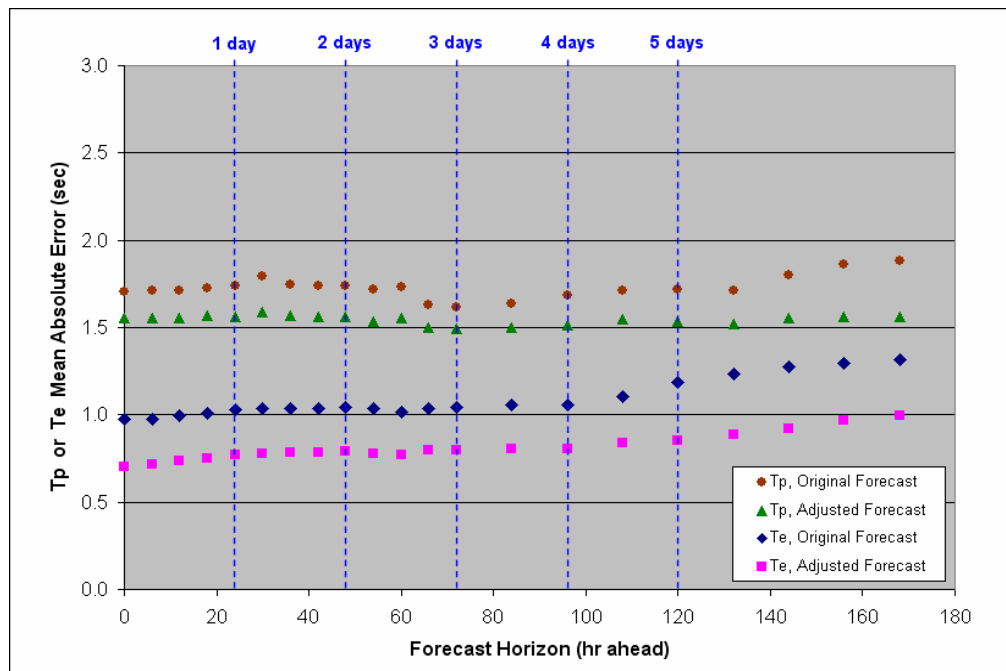


**Figure C-15.**  
Mean absolute error of WAVEWATCH III forecast for two wave period parameters at NDBC Station 46050 during the period from 24 May through 30 September 2007.



## Export Control Restrictions


Access to and use of EPRI Intellectual Property is granted with the specific understanding and requirement that responsibility for ensuring full compliance with all applicable U.S. and foreign export laws and regulations is being undertaken by you and your company. This includes an obligation to ensure that any individual receiving access hereunder who is not a U.S. citizen or permanent U.S. resident is permitted access under applicable U.S. and foreign export laws and regulations. In the event you are uncertain whether you or your company may lawfully obtain access to this EPRI Intellectual Property, you acknowledge that it is your obligation to consult with your company's legal counsel to determine whether this access is lawful. Although EPRI may make available on a case-by-case basis an informal assessment of the applicable U.S. export classification for specific EPRI Intellectual Property, you and your company acknowledge that this assessment is solely for informational purposes and not for reliance purposes. You and your company acknowledge that it is still the obligation of you and your company to make your own assessment of the applicable U.S. export classification and ensure compliance accordingly. You and your company understand and acknowledge your obligations to make a prompt report to EPRI and the appropriate authorities regarding any access to or use of EPRI Intellectual Property hereunder that may be in violation of applicable U.S. or foreign export laws or regulations.

## The Electric Power Research Institute (EPRI)

The Electric Power Research Institute (EPRI), with major locations in Palo Alto, California, and Charlotte, North Carolina, was established in 1973 as an independent, nonprofit center for public interest energy and environmental research. EPRI brings together members, participants, the Institute's scientists and engineers, and other leading experts to work collaboratively on solutions to the challenges of electric power. These solutions span nearly every area of electricity generation, delivery, and use, including health, safety, and environment. EPRI's members represent over 90% of the electricity generated in the United States. International participation represents nearly 15% of EPRI's total research, development, and demonstration program.

Together...Shaping the Future of Electricity

© 2007 Electric Power Research Institute (EPRI), Inc. All rights reserved.  
Electric Power Research Institute, EPRI, and TOGETHER SHAPING  
THE FUTURE OF ELECTRICITY are registered service marks of the  
Electric Power Research Institute, Inc.

 Printed on recycled paper in the United States of America

10xxxxx

---

### ELECTRIC POWER RESEARCH INSTITUTE

3420 Hillview Avenue, Palo Alto, California 94304-1338 • PO Box 10412, Palo Alto, California 94303-0813 • USA  
800.313.3774 • 650.855.2121 • [askepri@epri.com](mailto:askepri@epri.com) • [www.epri.com](http://www.epri.com)